Evaluation of Isoprene Nitrate Chemistry in Detailed Chemical Mechanisms

Alfred W. Mayhew[1], Ben H. Lee[2], Joel A. Thornton[2], Thomas J. Bannan[3], James Brean,[4] James R. Hopkins[1,5], James D. Lee[1,5], Beth S. Nelson[1], Carl Percival[3], Andrew R. Rickard[1,5], Marvin D. Shaw[1,5], Peter M. Edwards[1], Jaqueline F. Hamilton[1]

[1]Wolfson Atmospheric Chemistry Laboratories, Department of Chemistry, University of York, Heslington, York, UK
[2]Department of Atmospheric Sciences, University of Washington Seattle, Washington 98195, USA
[3]School of Earth and Environmental Sciences, University of Manchester, Manchester, UK
[4]School of Geography, Earth and Environmental Sciences, University of Birmingham, Birmingham, U.K.
[5]National Centre for Atmospheric Science, University of York, York, UK

Correspondence to: Jaqueline F. Hamilton (jacqui.hamilton@york.ac.uk)

Abstract. Isoprene nitrates are important chemical species in the atmosphere which contribute to the chemical cycles that form ozone and secondary organic aerosol (SOA) with implications for climate and air quality. Accurate chemical mechanisms are important for the prediction of the atmospheric chemistry of species such as isoprene nitrates in chemical models. In recent years, studies into the chemistry of isoprene nitrates have resulted in the development of a range of mechanisms available for use in the simulation of atmospheric isoprene oxidation. This work uses a 0-D chemical box-model to assess the ability of three chemically detailed mechanisms to predict the observed diurnal profiles of four groups of isoprene-derived nitrates in the summertime in the Chinese Megacity of Beijing. An analysis of modelled $C_5H_9NO_5$ isomers, including isoprene hydroperoxy nitrate (IPN) species, highlights the significant contribution of non-IPN species to the $C_5H_9NO_5$ measurement, including the potentially large contribution of nitrooxy hydroxyepoxide (INHE). The changing isomer distribution of isoprene hydroxy nitrates (IHN) derived from OH-initiated and NO_3-initiated chemistry is discussed, as is the importance of up-to-date alkoxy radical chemistry for the accurate prediction of isoprene carbonyl nitrate (ICN) formation. All mechanisms ~~reasonably reproduced~~under-predicted $C_4H_7NO_5$ as predominately formed from the major isoprene oxidation products, methyl vinyl ketone (MVK) and methacrolein (MACR). ~~–~~This work explores the current capability of existing chemical mechanisms to accurately represent isoprene nitrate chemistry in urban areas significantly impacted by anthropogenic and biogenic chemical interactions~~,~~. It suggests considerations to be taken when ~~applying these mechanisms to~~investigating isoprene nitrates in ambient scenarios, investigates the potential impact of varying isomer distributions on iodide chemical ionisation mass spectrometry (I⁻-CIMS) calibrations, and makes some proposals for the future development of isoprene mechanisms.

1 Introduction

Isoprene (2-methyl-1,3-butadiene) is the most emitted non-methane volatile organic compound (NMVOC) globally, and accounts for around 70% of global biogenic volatile organic compound (BVOC) emissions.(Guenther et al., 1995; Guenther et al., 2006; Guenther et al., 2012; Sindelarova et al., 2014) Isoprene is a dialkene, and so is susceptible to oxidation in the atmosphere, initiated by the breaking of one, or both, of the double bonds.(Wennberg et al., 2018) Some of the products of these reactions are organonitrates which are formed either by the reaction of isoprene with hydroxyl radicals (OH) and subsequent reactions with O_2 and NO, or by the addition of the nitrate radical (NO_3) to one of isoprene's double bonds. The resulting nitrates are important for their influence on the NO_x, HO_x, and O_3 budgets, as well as the potential for the formation of secondary organic aerosol (SOA) by condensation or via further reactions.(Emmerson and Evans, 2009; Bates and Jacob, 2019; Schwantes et al., 2019; Schwantes et al., 2020; Vasquez et al., 2020; Palmer et al., 2022)

This work focusses on three types of primary nitrates resulting from isoprene oxidation, and one group of secondary nitrates. The primary C_5 nitrates are the isoprene hydroxynitrates (IHN, Figure 1), isoprene carbonyl nitrates (ICN, Figure 2), and isoprene hydroperoxynitrates (IPN, Figure 3). The molecular formulae of IHN, ICN, and IPN are $C_5H_9NO_4$, $C_5H_7NO_4$, and $C_5H_9NO_5$, respectively. Throughout this work an upper-case sigma is used to denote the group of nitrates as well as any other species present in a chemical mechanism with the same molecular formula. For example, ΣIHN will refer to all isoprene hydroxynitrates as well as any other $C_5H_9NO_4$ species present in each chemical mechanism. A glossary of the terms used to refer to different nitrated species is given in the supplementary information (Table S4).

IHN may be formed by OH-initiated oxidation followed by a peroxy radical (RO_2) + NO reaction, or by NO_3-initiated oxidation followed by RO_2 cross-reactions to form the alcohol group (Figure 1). ICN is formed by NO_3-initiated oxidation followed by RO_2 cross-reactions, hydrogen abstraction from alkoxy radicals (RO) by oxygen (RO + O_2 → ICN + HO_2), or the reaction of IPN or isoprene dinitrates (IDN) with OH (Figure 2). IPN is formed by NO_3-initiated oxidation followed by RO_2 + HO_2 reactions (Figure 3).(Jenkin et al., 2015; Wennberg et al., 2018; Novelli et al., 2021; Vereecken et al., 2021)

The final group of nitrates are secondary nitrates with the formula $C_4H_7NO_5$, corresponding to the hydroxycarbonyl nitrate structures shown in Figure 4, which have been shown to be a major contributor to isoprene nitrates as measured by iodide chemical ionisation mass spectrometry (I⁻-CIMS).(Tsiligiannis et al., 2022 (under review))(Tsiligiannis et al., 2022) ΣC_4H_7NO_5 refers to the isoprene-derived nitrates as well as isomeric species present in the Master Chemical Mechanism (MCM) from other VOC sources.(Jenkin et al., 2015) There are several identified formation routes of $C_4H_7NO_5$ including the OH-initiated oxidation of methyl vinyl ketone (MVK) and methacrolein (MACR); NO_3-initiated oxidation of MVK and MACR; OH-initiated oxidation of IHN, IPN, and ICN; the ozonolysis of IHN; and the NO_3-initiated oxidation of hydroxycarbonyls (Figure 5).(Jenkin et al., 2015; Praske et al., 2015; Schwantes et al., 2015; Wennberg et al., 2018; Tsiligiannis et al., 2022 (under review))) Analysis of these multifunctional compounds is further complicated due to its secondary nature, as well as their potentially long atmospheric lifetime.(Müller et al., 2014)

Isoprene nitrates are often identified as major products of isoprene oxidation. For example, studies performed in the Forschungszentrum Jülich SAPHIR chamber identified a large range of organonitrates resulting from the NO_3-initiated oxidation of isoprene, including the primary products mentioned here.(Wu et al., 2021; Brownwood et al., 2021) Chamber experiments performed at the California Institute of Technology have also highlighted the role of nitrates in the OH-initiated oxidation of isoprene.(Schwantes et al., 2019; Vasquez et al., 2020) Such nitrates have also been identified in a range of ambient environments, from rural environments such as those in the south eastern United States, to polluted urban environments such as the San Francisco Bay area.(Ayres et al., 2015; Zaveri et al., 2020) Previous modelling studies that investigate isoprene nitrates under ambient conditions, and their impacts on atmospheric chemistry, are also widespread across polluted and less polluted environments, examining both speciated nitrates and the sum of total organic nitrates.(Pratt et al., 2012; Xiong et al., 2015; Romer et al., 2016; Chen et al., 2018; Zare et al., 2018; Schwantes et al., 2020)

Isoprene nitrates have also been identified as significant species during the 2017 Atmospheric Pollution and Human Health in a Chinese Megacity (APHH) summer campaign in Beijing.(Hamilton et al., 2021; Newland et al., 2021) There have been two previous box-modelling investigations focussed on the data collected during the APHH-Beijing intensive field observations.(Reeves et al., 2021; Whalley et al., 2021) Whalley *et al.* focussed on radical chemistry and ozone formation, highlighting several inconsistencies between modelled radical species and relevant measurements. Reeves *et al.* investigated IHN and ICN speciation and demonstrated the value of speciated measurements of isoprene nitrates by identifying several instances where the modelled IHN isomer distribution was not consistent with their measured distribution. They also discussed issues around the simplified representations of ICN isomers with regards to the initial site of attack of NO_3 and the E/Z stereochemistry of 1,4-ICN and 4,1-ICN. This paper uses similar box-modelling approaches as the previously discussed studies to assess the capabilities of three detailed atmospheric oxidation mechanisms for investigating the formation and losses of isoprene derived nitrates in this anthropogenically and biogenically impacted environment. Key statistics for each mechanism are given in Table S1.

The first mechanism used here is the Master Chemical Mechanism v3.3.1 (MCM).(Jenkin et al., 2015) The MCM is a benchmark near-explicit chemical mechanism extensively used by the atmospheric science community in a wide variety of science and policy applications where chemical detail is required. Subsets of the MCM can be directly extracted for a wide variety of VOCs (mcm.york.ac.uk). However, due to the breadth of the MCM, some simplifications have been made when constructing the mechanism. The first major simplification is the use of lumped RO_2 reactions. This means that RO_2-RO_2 cross-reactions are not treated explicitly, and it is assumed that each RO_2 will react with any other RO_2 at the same rate, which helps to greatly reduce the complexity of mechanisms.(Jenkin et al., 1997) In the case of isoprene, further assumptions are made. For example, NO_3-initiated oxidation of isoprene in the MCM is represented by only one isomer (NISOPO2).

Secondly, the full v5 isoprene oxidation mechanism taken from the Wennberg *et al.* 2018 review of gas-phase isoprene oxidation (henceforth, the Caltech Mechanism) was used.(Wennberg et al., 2018) This mechanism treats isoprene RO_2 cross-reactions explicitly, unlike the lumped-RO_2 approach of the MCM. This leads to issues when integrating the Caltech Mechanism with the MCM subset for additional measured VOCs, as explained further in the methodology section. The

Caltech Mechanism aims to provide a more up-to-date representation of reaction rates and products. For example, the Caltech Mechanism provides four different nitrated RO_2 radicals resulting from NO_3 oxidation. The Caltech Mechanism also introduces some reactions that are not found in the MCM, such as intramolecular RO_2 reactions.

130 Finally, the mechanism developed by Vereecken *et al.* and further expanded in Tsiligiannis *et al.* was used and is referred to as the FZJ Mechanism.(Vereecken et al., 2021; Tsiligiannis et al., 2022 ~~(under review)))~~ ~~This mechanism aims to expand on the Caltech Mechanism, by providing more comprehensive NO₃ chemistry, including the proposed formation of epoxide species from some alkoxy radical species, and additional chemistry relevant to C₄H₇NO₅ outlined in Tsiligiannis *et al.*(Tsiligiannis et al., 2022 (under review))~~ This mechanism aims to expand on the Caltech Mechanism, by providing more

135 comprehensive NO_3 chemistry, including the proposed formation of epoxide species from some alkoxy radical species, and additional chemistry relevant to $C_4H_7NO_5$ outlined in Tsiligiannis *et al.*(Tsiligiannis et al., 2022)

2 Methodology

2.1 Ambient Measurements

The Beijing measurements used in this work were collected at ground level at the Tower Section of the Institute of

140 Atmospheric Physics (IAP) in Beijing, China, between ~~2021~~2017-06-01 and ~~2021~~2017-06-18.(Shi et al., 2019) The nitrates were measured using a Filter Inlet for Gases and Aerosols (FIGAERO) coupled to a time-of-flight iodide chemical ionisation mass spectrometer (I⁻-CIMS) which allows for the measurement of particle and gas-phase species, although only the gas-phase data are used here as the particle-phase data were unavailable.(Lopez-Hilfiker et al., 2014) Each nitrate was calibrated assuming the same sensitivity as ~~IEPOX~~trans-beta-IEPOX, though the potential role of calibration on the measured nitrate

145 concentrations is discussed throughout this work.(Hamilton et al., 2021) Other organic compounds were measured by proton transfer mass spectrometry (PTR-MS), selected ion flow tube mass spectrometry (SIFT-MS), ~~comprehensive two dimensional gas chromatography with flame ionisation detection (GC×GC FID),~~ and dual-channel gas chromatography with flame ionization detection (DC-GC-FID).(Hopkins et al., 2011; ~~Dunmore et al., 2015;~~ Huang et al., 2016; Shi et al., 2019; Reeves et al., 2021) The sum of monoterpenes measured by PTR-MS and SIFT-MS was used to constrain alpha-pinene and

150 limonene in the models, assuming each compound comprised 50% of the total monoterpenes. Instruments used to measure organic species are summarised in Table S2 and the details of the instruments used to measure additional compounds can be found elsewhere.(Whalley et al., 2010; Whalley et al., 2018; Zhou et al., 2018; Shi et al., 2019; Hamilton et al., 2021; Whalley et al., 2021) Where species constraints were required in the modelling, and multiple measurements were taken, the mean of all of the measurements was used. The scanning mobility particle sizer (SMPS) instruments used to calculate

155 particle surface area as outlined in ~~the Results and Discussion section~~Section 2.3.1 are described in the Supplementary Information.

4

2.2 Mechanisms

This investigation involved a comparison of three different isoprene oxidation mechanisms. The MCM subset for isoprene and the additional VOCs which were measured throughout the campaign and were available in the MCM (Table S2) was extracted directly from the MCM website (mcm.york.ac.uk).(Jenkin et al., 2015) The MCM inorganic chemistry scheme was used for all three mechanisms.

The Caltech Mechanism was integrated with the MCM subset for the additional VOCs by producing lumped RO_2 cross-reactions ~~by averaging the rates of all cross-reactions for a specific RO_2 species. This approach assumes that the reaction of each isoprene RO_2 with any other RO_2 will proceed at the average rate of each isoprene RO_2 cross reaction described in the Caltech Mechanism~~using the approach outlined in Jenkin *et al.*(Jenkin et al., 1997) For each RO_2 species where explicit reactions are given, the geometric mean of the self-reaction rate and the CH_3O_2 self-reaction rate was used. If a self-reaction was not specified, then the CH_3O_2 self-reaction rate was used. Branching ratios were then applied to the alcohol-forming, carbonyl-forming, and alkoxy-forming reactions according to Jenkin *et al*.

The FZJ Mechanism was produced by adding the reactions outlined in Tsiligiannis *et al.* to the mechanism provided in Vereecken *et al*. and combining it with the MCM subset for measured non-isoprene species. (Vereecken et al., 2021; Tsiligiannis et al., 2022 ~~(under review))~~)

Each of the mechanisms used in this work have been made available online (doi.org/10.15124/500474f7-6e69-47db-baf7-36310451fd15).

2.3 Modelling Approach

AtChem2, an open-source zero-dimensional box-model tool, was used in this work.(Sommariva et al., 2019) A separate model was run for each day to avoid compounding errors carrying across multiple days of the model, for example the uncertainty that may result from imperfect accounting for physical processes. NO_2, O_3, CO, SO_2, HONO, and formaldehyde, along with ~~40~~29 primary VOCs for which data were available (Table S2), were all constrained to the 30-minute averaged measured values throughout the campaign. NO was left unconstrained due to the potential for local NO emissions to result in mixing ratios unrepresentative of the larger area that is important for the formation of long-lived organic products such as organonitrates. Constraining to NO would result in unrealistically low NO_3 concentrations by increasing the rate of the NO_3 + NO reaction based on elevated NO concentrations. Temperature, pressure, boundary-layer height, and relative humidity were also constrained to measured values. Photolysis values in the models were constrained to measured values where available (J_{O1D}, J_{NO2}, J_{HONO}, J_{HCHOr}, J_{HCHOnr}, $J_{NO3toNO}$, $J_{NO3toNO2}$, J_{CH3CHO}, $J_{CH3OCH3}$), and remaining photolysis rates were calculated according to the parameterization used in the MCM and scaled based on the ratio of the calculated and measured J_{NO2}. The models consisted of a 24-hour spin-up period followed by a further 24-hour period. Constraints were made by duplicating the measured values for each day to provide a 48-hour constraint of two repeated 24-hour periods. The model

output was then considered to be the model output in the second 24-hour period of the model run. The model outputs were
220   then concatenated to produce a time series across the whole period of interest.

To account for the deposition of species to surfaces, deposition reactions were added for all species. Each species was assigned a deposition velocity based on the functionality of that compound. Deposition velocities for H_2O_2, HNO_3, and O_3 were applied directly to each compound. Separate deposition velocities for organic hydroperoxides and organic nitrates were applied to compounds containing the hydroperoxide and nitrate functional groups. Organic acid species were assigned the
225   formic acid deposition velocity, and a general oxidised VOC deposition was assigned to carbonyl and alcohol containing compounds. ~~For multifunctional compounds, the largest deposition velocity was selected.~~ The rate of deposition was determined by ~~multiplying~~dividing the assigned deposition velocity by the measured boundary layer height. All deposition velocities were taken from Nguyen *et al.* 2015 and are summarised in Table S3.(Nguyen et al., 2015) For multifunctional compounds, the largest deposition velocity of each of the functional groups present in the compound was selected from
230   Table S3.

Additionally, a loss term was included for all species to account for mixing and ventilation. ~~Since the magnitude of the~~ A diurnally varying ventilation rate ~~is highly uncertain, a~~ was applied, where the rate ~~of 1.157×10^{-5} s^{-1} was given for all species, resulting~~was scaled such that the modelled glyoxal concentrations matched measurements, in a ~~lifetime with respect~~similar fashion to ~~ventilation of 24 hours.~~previous work. (Whalley et al., 2021; Reeves et al., 2021) The sensitivity of
235   the model results to this term is assessed in the Model Validation section.

2.3.1 Particle Phase Processes

In the cases of ΣIHN and ΣIPN, an analysis of the impact of the particle-phase hydrolysis of 1,2-IHN and the reactive uptake of INHE is performed. For both of these cases, the rates of loss (k_{IHN} and k_{IHNE} for IHN hydrolysis and INHE uptake respectively) are calculated using Equation 1. S_a is the aerosol surface area, as calculated for each model time-step from
240   scanning mobility particle sizer (SMPS) measurements, r_p is the effective particle radius calculated as a weighted median of the SMPS number measurements at each model time-step, D_g is the gas-phase diffusion coefficient, v is the mean molecular speed of IHN or INHE molecules in the gas phase, and γ is the reactive uptake coefficient. v was calculated using Equation 2 where R is the ideal gas constant (8.314 J K^{-1} mol^{-1}), T is the measured temperature at each time-step, and M_r is the molecular mass of the compound of interest (0.147 kg mol^{-1} for IHN and 0.163 kg mol^{-1} for INHE). A value of 1×10^{-5} m^2 s^{-1}
245   was used for D_g, as is assumed in Gaston *et al.* for IEPOX. (Gaston et al., 2014) This method has been extensively used to calculate the rate of reactive uptake of IEPOX. (Gaston et al., 2014; Riedel et al., 2016; Budisulistiorini et al., 2017)

$$k_{IHN} = \frac{S_a}{\dfrac{r_p}{D_g} + \dfrac{4}{v\,\gamma_{IHN}}} \qquad\qquad Equation\ 1$$

$$v = \sqrt{\frac{3\,R\,T}{M_r}} \qquad\qquad Equation\ 2$$

An estimation of γ is complicated by the dependence on particle properties. In each case, results are shown for models where a range of γ values are assumed, between the limits of 0 and 1.

3 Results and Discussion

3.1 Model Validation

When comparing the measured and modelled NO mixing ratios, there is good agreement during the day-time, with the models deviating from the measurement by a maximum of around 2 times (Figure 6a). The models do not reproduce the elevated night-time NO concentrations observed in Beijing, however this night-time NO is likely the result of local emissions and so will have little impact on the chemistry that is the focus of this study. Figure S1 shows the good match between modelled NO and NO measured at an altitude of 100m showing the ability of the model to predict NO away from local sources. This is further confirmed by NO_3 predictions provided by the models being, at most, 2.5 times over-predicted (Figure 6b). There is also a slight under-prediction of NO_3 by a factor of around 0.4 during the afternoon.

HO_x predictions from the models are generally good. There is close agreement to the measured OH concentrations, although the modelled concentrations are around 0.5 times the measured values during the morning period (Figure 6c). Day-time HO_2 concentrations are around 2 times higher than the measurement during the evening in all models (Figure 6d), which is consistent with findings from Whalley *et al.* 2021 where a similar box-model run using the MCM over-predicted HO_2, particularly during low-NO periods. Whalley *et al.* hypothesises that the HO_2 over-prediction may be caused by unaccounted for RO isomerisation reactions that result in RO_2 radical formation without concurrent HO_2 formation.(Whalley et al., 2021) While the Caltech Mechanism and FZJ Mechanism both include additional RO isomerisation reactions for isoprene, they inherit the MCM RO chemistry for other VOCs, including longer-chain VOCs that may be more susceptible to RO isomerisations, and so this could still be a reasonable hypothesis. The major contributors to RO composition in the models are aromatic species owing to their relatively long lifetimes.

When comparing the modelled and measured MVK and MACR mixing ratios, while ~~the models~~day-time concentrations are ~~within the uncertainty~~at-most half of the measured values, the night-time concentrations fall far below the measurements ~~during the night, there is an over-prediction of around 3 times during the day across all models~~ (Figure S2). This ~~is likely~~may be the result of the long lifetime of MVK and MACR, meaning there is a high background concentration not captured by the models. Alternatively, it may due to imperfect accounting for physical processes such as mixing and ventilation within the models~~, though there could also be contributions resulting from~~ or a poor understanding of ~~the~~ MVK+MACR chemistry in this environment. There may also be some role played by the conversion of isoprene hydroxyhydoperoxides to MVK+MACR on the metal inlets of the mass spectrometers resulting in an artificially increased measurement. (Rivera-Rios et al., 2014; Newland et al., 2021) It is also important to consider the effect of upwind isoprene concentrations for all of the isoprene oxidation products discussed in this work. While our modelling makes use of isoprene concentrations measured at

the same site as the product measurements, the upwind isoprene concentrations would be more useful for predicting the concentrations of isoprene oxidation products.

While a ventilation term is included in the models, and is scaled to glyoxal concentrations, there is a large uncertainty as to its true rate and diurnal variability. As a test of the models' sensitivity to the ventilation rate, the rate was halved and doubled in two separate tests (Figure S3). The halving of the ventilation rates resulted in an average change in concentration across the models run with each mechanism of 15%, 6%, 3.1, 1.5, 1.8%,. and 9%1.8 times for $\Sigma C_4H_7NO_5$, ΣIHN, ΣICN, and ΣIPN respectively. The average changes for doubling the ventilation rate were 40%, 12%, 17%,0.32, 0.62, 0.60, and 19%0.56 for $\Sigma C_4H_7NO_5$, ΣIHN, ΣICN, and ΣIPN respectively. Xiong *et al.* aimed to reduce the impact of ventilation by analysing nitrates as ratios with the sum of MVK and MACR.(Xiong et al., 2015) However, due to the differences in MVK+MACR predicted using each mechanism, using the MVK+MACR ratio as a proxy for the absolute concentration of the nitrates complicates the comparison of different mechanisms. As such, the analysis here primarily involves the use of mixing ratios as opposed to the ratios relative to MVK+MACR. In order to analyse the average trends over a day within the modelled period, average diurnal plots are used to examine the modelled and measured data. The mean diurnals are used here, though use of the median had little impact on the diurnal values.

Comparison of the MVK+MACR predicted using each mechanism is consistent with the work presented in Vereecken *et al*. (Vereecken et al., 2021) Figure S2 shows that the Caltech Mechanism produces the highest night-time MVK+MACR concentrations with the MCM and FZJ Mechanism producing the lowest night-time concentrations. The MCM does not include MVK+MACR formation from isoprene+NO_3 chemistry, while the Caltech Mechanism does. The FZJ Mechanism does include some MVK+MACR formation from isoprene NO_3 chemistry, but also reduces the yield from ozonolysis reactions resulting in similar MVK+MACR yields between the MCM and FZJ Mechanism in Vereecken *et al.* and in the night-time period of the models presented here. During the day-time, the FZJ models produce the lowest MVK+MACR concentrations as this adjusted ozonolysis chemistry becomes more significant.

Isoprene epoxydiols (IEPOX) are a significant contributor to isoprene-derived SOA and are significant isoprene oxidation products along with the isobaric isoprene hydroxyhydoperoxides (ISOPOOH).(Paulot et al., 2009; Surratt et al., 2010; Nguyen et al., 2014) Figure S4 shows the modelled and measured $\Sigma IEPOX+ISOPOOH$. All three mechanisms show a similar trend relative to the measurement as is seen for MVK+MACR (Figure S2), with an over-prediction of approximately 1.25 times in the afternoon and a significant under-prediction in the morning. This large under-prediction in the morning may result from the under-prediction of OH in the morning period or another missing source. Since the reactive uptake of IEPOX to acidified particles is not included in these models, it seems likely that the issue is the result of an under-prediction of the formation rate of IEPOX and not an over-prediction of the lossesAll three mechanisms resulted in a large under-prediction of $\Sigma IEPOX+ISOPOOH$. As with MVK+MACR, this under-prediction may result from ventilation from the model being too rapid. As discussed throughout the manuscript, there may also be an issue of calibration for the I$^-$-CIMS data. Although the I$^-$-CIMS data is calibrated using IEPOX, all three models predict around half of the $\Sigma IEPOX+ISOPOOH$ to be comprised of ISOPOOH. Accounting for particle-uptake of IEPOX would only increase this fraction of ISOPOOH. Additionally, there are

8

multiple IEPOX isomers whereas this data is calibrated to only one isomer. More discussion of calibration issues is given in Section 3.2.1.

315   The volatility of the nitrate species was assessed in order to determine the potential impact of condensation to the particle phase. An equilibrium partitioning approach was taken, as described in Mohr *et al.* 2019.(Mohr et al., 2019) This resulted in common logarithm of saturation concentrations in units of molecules cm^{-3} (log(C_{sat})) of between 4.0 and 5.3, revealing the high volatility of these compounds. As such, the condensation of these nitrates to the particle phase is assumed to be negligible, though this approach does not account for reactive uptake to particles.

320   **3.2 ΣIHN ($C_5H_9NO_4$)**

Throughout the day, the three mechanisms produce similar ΣIHN mixing ratios, at approximately half of the measured value (Figure 7). Despite the absolute differences, the profile of modelled ΣIHN matches the measurement, with decreasing mixing ratios in the afternoon reflecting the titration of NO by increasing O_3. (Newland et al., 2021) Reeves *et al.* shows reasonable predictions of the major IHN isomer (1,2-IHN) made by their MCM-based model, whereas the modelled 4,3-IHN showed an

325   over-prediction of around two times at mid-day.(Reeves et al., 2021) This discrepancy is likely the result of different representations of physical processes in the models. The time series for modelled and measured ΣIHN is shown in Figure S5. Figure 8 shows the clear split between the day-time and night-time IHN speciation in all of the models. Figure 8 also demonstrates that the contribution of non-IHN species to ΣIHN in the models is very small, meaning a measured ΣIHN ($C_5H_9NO_4$) signal is likely to be a reasonable measurement of IHN. Both OH and NO_3 addition to isoprene favours the

330   terminal carbon atoms, so OH oxidation followed by reaction with NO results in the nitrate group being formed either on one of the central positions or the remaining terminal carbon. This means OH-initiated oxidation predominantly forms 1,2-IHN, 4,3-IHN, E/Z-1,4-IHN, and E/Z-4,1-IHN. NO_3 addition results in the nitrate group being present on the terminal carbons, at the initial site of attack.(Wennberg et al., 2018) This means NO_3-initiated oxidation predominantly forms 2,1-IHN, 3,4-IHN, E/Z-1,4-IHN, and E/Z-4,1-IHN.

335   The night-time shows an enhancement in IHN species produced by NO_3 chemistry. This is most obvious in the MCM model, where all isoprene + NO_3 chemistry is channelled through just one isomer, ISOPCNO3. As such, ISOPCNO3 makes up very little of the day-time IHN, but up to 80% of night-time IHN just before sunrise. Similarly, the ΣIHN modelled using the Caltech Mechanism and FZJ Mechanism are almost exclusively comprised of ISOP1OH2N and ISOP3N4OH during the day, but there is a more even distribution at night with major contributions from ISOP1N2OH, ISOP1N4OHt, and

340   ISOP1N4OHc. The FZJ Mechanism contains a reduced rate of ISOP1N2OH formation from ISOP1N2OO cross-reactions compared to the Caltech Mechanism, hence the lower contribution of 'NO$_3$-initiated IHN' to ΣIHN in the FZJ Mechanism model.

Previous work has shown that the hydrolysis of 1,2-IHN occurs rapidly in the atmosphere.(Vasquez et al., 2020; Liu et al., 2012) To test the sensitivity of our results to 1,2-IHN hydrolysis, loss reactions of 1,2-IHN were added to each of the

345   mechanisms with a rate calculated as described in Section 2.3.1. Figure S6 shows the modelled ΣIHN using each of the

9

mechanisms with 1,2-hydrolysis reactions included. Since the majority of daytime ΣIHN is comprised of 1,2-IHN, removal
of this compound can have a large effect on the modelled ΣIHN. A γ_{IHN} value of 1 removes most, but not all, of the 1,2-IHN
and a value of 0.1 brings modelled ΣIHN concentrations close to when the value is 1. Conversely, γ_{IHN} values below 0.01
only result in small changes to modelled ΣIHN compared to the base model where no IHN hydrolysis is included.

3.2.1 ΣIHN Calibration

As previously noted, the I⁻-CIMS data presented here is calibrated relative to IEPOX, which results in two potential issues.
Firstly, the sensitivity of I⁻-CIMS to the compounds of interest may be significantly different from the sensitivity to IEPOX,
leading to a bias in the measurement. Secondly, if I⁻-CIMS has different sensitivities to the different isomers of a particular
formula, the changing isomer distribution over time will result in a varying sensitivity to the entire m/z signal as each isomer
contributes more or less. For example, it has been previously shown that I⁻-CIMS is more sensitive to IHN isomers in which
the NO_3 group is located close to the OH group, such as 4,3-IHN and Z-1,4-IHN. Isomers where the NO_3 and OH groups
are not in close proximity, such as E-1,4-IHN, show much lower responses to iodide-adduct ionisation. (Lee et al., 2014) The
"Mixed-source IHN" in Figure 8 includes both E and Z isomers of 1,4-IHN and 4,1-IHN. Since there is a higher proportion
of mixed-source IHN during the night in all models, the sensitivity of ΣIHN can be expected to be lower at night than during
the day due to a higher proportion of E-1,4-IHN and E-4,1-IHN.

Lee *et al.* report sensitivity values for IEPOX alongside the sensitivity values for three IHN isomers (4,3-IHN, Z-1,4-IHN,
and E-1,4-IHN).(Lee et al., 2014) Dividing the sensitivities of each of these isomers by the IEPOX sensitivity allows a
relative sensitivity to be obtained for each. These relative sensitivities are 15.64, 14.62, and 0.9487 for 4,3-IHN, Z-1,4-IHN,
and E-1,4-IHN respectively. Relative sensitivities for the remaining IHN isomers can be assigned based on the orientation of
the OH and NO_3 groups.(Xiong et al., 2015) A total ΣIHN sensitivity can then be estimated using the modelled isomer
distribution from each set of models. Figure 9a shows the diurnally varying relative sensitivity for each of the models. The
largest discrepancy between the models can be seen at night, resulting from the differing NO_3 chemistry in each mechanism.
Taken together, the models indicate that I⁻-CIMS may be between 2.5 to 1.4 times less sensitive to ΣIHN during the night
than during the day.

Applying this relative ΣIHN sensitivity to the IEPOX calibrated data dramatically reduces the measured concentrations of
ΣIHN, due to the high sensitivities of the majority of IHN isomers (Figure 9b). It is interesting to note differing ΣIHN
concentrations predicted using the isomer distribution from each mechanism. At midnight, the FZJ-adjusted ΣIHN data is
around twice that of the Caltech-adjusted data. According to this adjusted ΣIHN data, all of the models would be over-
predicting ΣIHN by around an order of magnitude. Even when comparing to the most extreme 1,2-IHN hydrolysis case
previously presented, ΣIHN concentrations are over-predicted by 1.5 to 3 times compared to the adjusted I⁻-CIMS data.
Additionally, the adjusted calibration factors change the shape of the ΣIHN diurnal, resulting in a second peak in mixing
ratios at around 20:00. Using the isomer distribution predicted by the FZJ mechanism suggests that this second night-time
peak could be as large as the mid-day peak.

10

The use of relative responses here aims to eliminate some issues associated with the direct comparison of data from different instruments, but may not eliminate all of the unknown differences. Nevertheless, adjusting the measured ΣIHN in this way suggests that the perceived under-prediction in ΣIHN by all of the models may instead be a closer representation to the true ΣIHN concentrations, if not an over-prediction. IHN is the most widely studied of the nitrates presented here and so the calibration correction can be applied quantitatively, however the impact of calibration on the measured organonitrate concentrations must be considered throughout this work.

3.3 ΣIPN ($C_5H_9NO_5$)

The measured ΣIPN shows little diurnal variation (Figure 10). Contrary to observations, all models produced strong diurnal profiles of ΣIPN. This is because the majority of IPN is formed through NO_3 oxidation of isoprene at night when there are few losses. The only losses of IPN in all mechanisms, besides the added deposition reactions, are photolysis reactions and the reaction with OH, which are day-time processes, resulting in no night-time loss routes. The Caltech Mechanism produces the lowest ΣIPN mixing ratios, though the. The strong diurnal profile results in night-time mixing ratios being over-predicted by around 1.755 times and day-time mixing ratios being aroundclose to 0.25 times the measured value. Both the MCM and FZJ Mechanism result in ΣIPN reaching a minimum at sunrise, graduallyslightly increasing throughout the day, before a rapid night-time increase. The daytime under-prediction of ΣIPN may be indicative of mixing in the models being overestimated. The time series for modelled and measured ΣIPN is shown in Figure S5S7. The data presented in Figure S7 show that there is substantial noise in the ΣIPN data, which may also mask diurnal trends and indicates that the ΣIPN concentrations are close to the instrument's detection limit for these compounds.

While none of the mechanisms include NO_3 or O_3 oxidation of IPN, the Wennberg *et al.* 2018 review of isoprene chemistry does list estimated reaction rates of IPN, ICN, and IHN with NO_3, O_3, and OH. (Wennberg et al., 2018) Figure S8 shows the average proportional night-time chemical loss for IHN, IPN, and ICN calculated using the rates given in Wennberg *et al.* and the measured OH, O_3, and NO_3 concentrations between 20:00 and 05:00. For the IPN isomers, OH oxidation accounts for the majority of the chemical loss of IPN at night, with around 10-15% being lost to reaction with NO_3. Reaction with O_3 also makes up a substantial fraction of the chemical loss in the 1,4-IPN and 4,1-IPN isomers, though OH is still the major sink. Since OH oxidation is included in the mechanisms, then the majority of the chemical losses should be captured by the models. Physical processes also dominate the losses of ΣIPN at night, so the addition of more chemical losses would not have a large impact on ΣIPN concentrations.

To understand the trends in ΣIPN, it is important to consider the multiple isomeric (non-IPN) species present in each of the mechanisms which can make up a large proportion of the modelled ΣIPN (i.e. species with the formula $C_5H_9NO_5$). The most significant isomers of IPN are C51NO3, originally from the MCM and present in all mechanisms, C524NO3, originally from the MCM and also present in the FZJ mechanism, ISOP1N23O4OH, present in the Caltech Mechanism and FZJ Mechanism, and ISOP1N253OH4OH, present in the Caltech Mechanism (Figure S6S9).

11

C51NO3 is a nitrated hydroxy carbonyl compound in the MCM with formation routes from isoprene, as well as from hydrocarbons such as pentane. C524NO3 is an isoprene OH oxidation product from the MCM. In the MCM and FZJ Mechanism models, C51NO3 ~~makes~~and C524NO3 make up the majority of modelled ΣIPN composition during the day-time ~~and into the evening~~ (Figure ~~S7). This is~~ S10). These are the species responsible for the ~~gradual~~slight increase in ΣIPN throughout the day in the MCM and FZJ Mechanism models. C51NO3 and C524NO3 production from isoprene is not included in the Caltech Mechanism, and ~~so~~ the only formation routes to C51NO3 are from non-isoprene species. As such, C51NO3 and C524NO3 only makes a small contribution to total ΣIPN in the Caltech Mechanism model and the day-time increase is not present.

ISOP1N253OH4OH is only present in the Caltech Mechanism and is initially formed from an intramolecular H-shift of the 1,4 isoprene alkoxy nitrate (INO), ISOP1N4O. The Caltech Mechanism does not contain any loss reactions for this species, which may account for its ~~significant~~moderate contribution to modelled night-time ΣIPN (Figure ~~S7~~S10). This INO H-shift pathway is not included in the FZJ Mechanism and so ISOP1N253OH4OH is not present.

ISOP1N23O4OH is a nitrated hydroxyepoxide that was proposed, alongside other positional isomers which are produced by the models in lower amounts, as a product of IPN OH oxidation by Schwantes *et al.* where it is termed isoprene nitrooxy hydroxyepoxide (INHE).(Schwantes et al., 2015) While the formation of INHE from IPN is present in the Caltech Mechanism, epoxidation reactions from alkoxy radicals that are predicted in Vereecken *et al.* result in much more INHE production in the FZJ Mechanism model. The FZJ Mechanism model results predict that at midnight, around half of the total ΣIPN is composed of INHE (Figure 11). If such large concentrations of these epoxides are produced, then this could have a significant impact on SOA formation via reactive uptake in a similar fashion to IEPOX.(Paulot et al., 2009; Surratt et al., 2010; Schwantes et al., 2015; Hamilton et al., 2021)

In order to assess the potential for reactive uptake of INHE ~~to bring~~on the modelled ΣIPN ~~in line with measurements~~, loss reactions for each of the four INHE isomers in the FZJ Mechanism were added to the mechanism and the models rerun. The rate coefficient for the reactive uptake of INHE (k_{INHE}) was calculated ~~using Equation 1, where S_a is the aerosol surface area, as calculated for each model time step from scanning mobility particle sizer (SMPS) measurements, r_p is the effective particle radius calculated as a weighted median of the SMPS number measurements at each model time step, D_g is the gas-phase diffusion coefficient, ν is the mean molecular speed of INHE molecules in the gas phase, and γ_{INHE} is the reactive uptake coefficient of INHE. ν was calculated using Equation 2 where R is the ideal gas constant (8.314 J K^{-1} mol^{-1}), T is the measured temperature at each time step, and M_r is the molecular mass of INHE (0.16313 kg mol^{-1}~~as described in Section 2.3.1. Figure S11 shows the modelled ΣIPN produced by a set~~~~). A value of 1×10^{-5} m^2 s^{-1} was used for D_g, as is assumed in Gaston *et al.* for IEPOX. (Gaston et al., 2014) This method has been extensively used to calculate the rate of reactive uptake of IEPOX. (Gaston et al., 2014; Riedel et al., 2016; Budisulistiorini et al., 2017)~~

$$k_{INHE} = \frac{S_a}{\frac{r_p}{D_g} + \frac{4}{v\,\gamma_{INHE}}} \qquad\qquad \text{~~Equation 1~~}$$

475

$$v = \sqrt{\frac{3\,R\,T}{M_r}} \qquad\qquad \text{~~Equation 2~~}$$

~~An estimation of γ_{INHE} is complicated by the dependence on particle properties, but Figure S8 shows the modelled ΣIPN produced by a range~~ of models for which a range of γ_{INHE} were assumed, between the limits of 0 and 1. When γ_{INHE}=1 and γ_{INHE}=0.1, almost all of the INHE is removed from the gas-phase at any time which brings the modelled night-time concentrations of ΣIPN ~~closer to~~ around two thirds of the measured value~~, though there is still an over-prediction of around 2~~

480 ~~times in the early night time.~~. When γ_{INHE} = 0.01, the modelled night-time ΣIPN is ~~close to~~ reasonably in line with the measurements between 20:00 and 00:00, after which the modelled ~~value when~~ concentrations fall with the diurnal profile explained previously. γ_{INHE} = ~~1, whereas a γ_{INHE} of~~ 0.001 results in modelled concentrations close to the values without any particle uptake. Previous estimations of the reactive uptake coefficient of IEPOX (γ_{IEPOX}) usually range between 7×10^{-2} and 2×10^{-4}, though measurements have been made as low as 9×10^{-7}. (Gaston et al., 2014; Riedel et al., 2015; Budisulistiorini et

485 al., 2017) ~~As such, it is unlikely that the reactive uptake of INHE can explain the over prediction in night-time ΣIPN made by the FZJ model.~~

~~3.3 ΣIHN ($C_5H_9NO_4$)~~

~~Throughout the day, the three mechanisms produce similar ΣIHN mixing ratios, at approximately twice the measured value. Despite the absolute differences, the profile of modelled ΣIHN matches the measurement, with decreasing mixing ratios in~~

490 ~~the afternoon reflecting the titration of NO by increasing O_3.(Newland et al., 2021) The largest deviation between the models occurs at night, where the Caltech Mechanism produces a night time peak in ΣIHN which is not observed in the other models or the measurements (Figure 9). Furthermore, ΣIHN concentrations fall rapidly through the early morning in the MCM and Caltech Mechanism models while the FZJ Mechanism model is more consistent with the profile of the measurements as the ΣIHN mixing ratio remains stable between 00:00 and 06:00. Reeves et al. shows reasonable predictions~~

495 ~~of 1,2 IHN made by their MCM based model, however the modelled 4,3 IHN showed a similar trend to the ΣIHN from the MCM model shown here, with an over-prediction of around two times at mid day.(Reeves et al., 2021) The time series for modelled and measured ΣIHN is shown in Figure S9.~~

~~Figure 10 shows the clear split between the day time and night time IHN speciation in all of the models. Figure 10~~As with all of the nitrates investigated here, the role of the I$^-$-CIMS calibration on the data presented must be considered. As shown

500 previously, all models predict a diurnally varying isomer distribution with night-time ΣIPN being largely comprised of IPN and/or INHE, and daytime ΣIPN being comprised of smaller concentrations of other species. If the daytime isomers were much more sensitively detected than the night-time isomers then this could offset the diurnal concentration profile modelled to produce a constant measured signal throughout the day, as is observed. The daytime ΣIPN concentrations predicted by the

MCM and FZJ models is around 0.06 times the measured values, meaning that the daytime isomers would need to be around 17 times more sensitively detected than IEPOX to reproduce the flat diurnal signal observed, assuming the night-time

540 isomers had the same sensitivity as IEPOX. There has been very little research to quantify the sensitivity of I⁻-CIMS to hydroperoxides, but Lee *et al.* reported the sensitivity of peroxyacetic acid to be 0.04 times that of acetic acid suggesting that the non-hydroperoxide daytime nitrates may be more sensitively detected than the night-time IPN. also demonstrates that the contribution of non-IHN species to ΣIHN in the models is very small, meaning a measured ΣIHN (C₅H₉NO₄) signal is likely to be a reasonable measurement of IHN. Both OH and NO₃ addition to isoprene favours the terminal carbon atoms, so

545 OH oxidation followed by reaction with NO results in the nitrate group being formed either on one of the central positions or the remaining terminal carbon. This means OH-initiated oxidation predominantly forms 1,2-IHN, 4,3-IHN, E/Z-1,4-IHN, and E/Z-4,1-IHN. NO₃ addition results in the nitrate group being present on the terminal carbons, at the initial site of attack.(Wennberg et al., 2018) This means NO₃-initiated oxidation predominantly forms 2,1-IHN, 3,4-IHN, E/Z-1,4-IHN, and E/Z-4,1-IHN.

550 The night-time shows an enhancement in IHN species produced by NO₃ chemistry. This is most obvious in the MCM model, where all isoprene + NO₃ chemistry is channelled through just one isomer, ISOPCNO3. As such, ISOPCNO3 makes up very little of the day-time IHN, but up to 80% of night-time IHN just before sunrise. Similarly, the ΣIHN modelled using the Caltech Mechanism and FZJ Mechanism are almost exclusively comprised of ISOP1OH2N and ISOP3N4OH during the day, but there is a more even distribution at night with major contributions from ISOP1N2OH, ISOP1N4OHt, and

555 ISOP1N4OHc. The FZJ Mechanism contains a reduced rate of ISOP1N2OH formation from ISOP1N2OO cross-reactions compared to the Caltech Mechanism, hence the far lower contribution of 'NO₃-initiated IHN' to ΣIHN in the FZJ Mechanism model. This also helps to explain the elevated absolute night-time ΣIHN concentrations observed when using the Caltech Mechanism compared to using the FZJ Mechanism (Figure 9).

This composition difference offers potential for identifying the source of oxidation for isoprene impacted air masses. An air

560 mass dominated by 1,2- and 4,3-IHN likely results from OH oxidation, though differing rates of hydrolysis between IHN isomers would also alter this distribution.

Additionally, recognising this changing IHN composition profile could aid with the calibration of instruments that cannot distinguish between IHN isomers. The instrument response of an IHN measurement which cannot distinguish isomers necessitates an assumption as to the expected isomer distribution, since each ΣIHN isomer will have a different response.

565 Ideally, some consideration will be given to the different sensitivities of the instrument to different isomers.(Lee et al., 2014) However, it is difficult to obtain authentic standards for many of the species of interest. It has been previously shown that I⁻-CIMS is more sensitive to IHN isomers in which the NO3 group is located close to the OH group, such as 4,3-IHN and Z-1,4-IHN. Isomers where the NO3 and OH groups are not in close proximity, such as E-1,4-IHN, show much lower responses to iodide adduct ionisation. (Lee et al., 2014) While it may be convenient to assume a constant IHN ratio distribution

570 governed by that expected from OH oxidation, the recognition of changing IHN sources over the course of 24 hours implies the requirement for a varying calibration factor. The "Mixed source IHN" in Figure 10 includes E and Z isomers of 1,4 IHN

14

3.4 ΣICN ($C_5H_7NO_4$)

ΣICN shows the largest difference between mechanisms. In line with the measurements, all models show low concentrations of ΣICN during the day (Figure 12). ΣICN then increases at sunset, due to NO_3-initiated formation from isoprene, and then reduces in concentration into the early morning as production ceases. There is a large over-prediction of a factor of ~~≈35~~around 25 times in the night-time mixing ratio modelled using the MCM which is consistent with findings from Reeves *et al.* who also found ICN to be over-predicted in their models using the MCM, however the lack of NO constraint in our models results in slightly higher modelled ICN concentrations due to elevated NO_3 concentrations, hence the discrepancy between the model and measurement is slightly larger in this work.(Reeves et al., 2021) This over-prediction decreases to around ~~10~~7 times when using the Caltech Mechanism, and decreases further to around ~~4~~3 times when using the FZJ Mechanism. A plot of ΣICN concentrations normalised to the concentration at midnight is shown in Figure ~~S10. The time series for measured and modelled ΣICN is given in Figure S11. It is also important to consider that previous work has found the lower sensitivity to aldehyde and ketone groups by I⁻-CIMS compared to alcohols, as such it should be expected that the measured ΣICN is most likely to be under-quantified by use of the IEPOX calibrant compared to species such as IHN.(Lopez-Hilfiker et al., 2014; Iyer et al., 2016)~~S12. The time series for measured and modelled ΣICN is given in Figure S13.

The large over-prediction made by the MCM is the result of large production terms from the decomposition of all INO radicals (represented by NISOPO in the MCM) into ICN. In contrast, the Caltech Mechanism provides alternative INO decomposition routes including fragmentation and H-shift autoxidation reactions (Figure ~~S12~~S14). The FZJ Mechanism includes much of this updated chemistry as well as proposing the previously discussed epoxide formation reactions from some alkoxy radicals, which further reduces the ICN production route (Figure ~~S12~~S14). The improvement in predictions of ΣICN indicates that the assumption made by the MCM of 100% of INO decomposing to form ICN is unlikely to be valid. The loss of ΣICN is dominated by physical processes in all of the models, particularly at night when ΣICN concentrations are the highest. Additional ICN losses being added to the MCM may improve ΣICN predictions, for example Hamilton *et al.* proposed ICN as a precursor to particle-phase species observed in Beijing via an isoprene nitrooxy hydroxy-α-lactone (INHL) species.(Hamilton et al., 2021) However, the MCM already includes reactions with O_3 and NO_3 that are not included in the Caltech or FZJ Mechanisms, suggesting that the issue lies in the MCM's faster formation processes. Further discussion of the uncertainties in ICN losses is given by Reeves *et al.*(Reeves et al., 2021)

While this account of increasingly complex alkoxy radical chemistry gives good reason to question the high ICN formation rates from the MCM, it is also important to consider that previous work has found the lower sensitivity to aldehyde and

605 ketone groups by I⁻-CIMS compared to alcohols, as such it should be expected that the measured ΣICN is most likely to be under-quantified by use of the IEPOX calibrant compared to species such as IHN.(Lopez-Hilfiker et al., 2014; Iyer et al., 2016; Lee et al., 2014) For example, Lee *et al.* 2014 shows that the sensitivity to hydroxyacetone is around 20 times lower than the similarly structured 1,2-butanediol and the sensitivity to 2,5-hexanedione is around 70 times lower than that of 5-hydroxy-2-pentanone. Assuming the relative sensitivity of ICN to IEPOX is lower than that of IHN, i.e. the sensitivity

610 relative to IEPOX is lower than 15.64 (Section 3.2.1), would mean that the over-prediction made by the MCM could not be solely accounted for by the calibration. However, it is more difficult to comment on the accuracy of the FZJ mechanism compared to the Caltech mechanism in this respect as a reasonable calibration correction could bring the measurement in line with either model.

3.5 $\Sigma C_4H_7NO_5$

615 ~~Day-time $\Sigma C_4H_7NO_5$ mixing ratios are over-predicted in all models, while night-time mixing ratios are approximately in line with measurements (Figure 12a). This is broadly consistent with the differences between measured and modelled MVK and MACR (Figure S2). Since the models show that most of the $C_4H_7NO_5$ is formed during the day from MVK and MACR, analysing the $\Sigma C_4H_7NO_5$/(MVK+MACR) ratio will allow for the influence of the MVK+MACR over prediction to be minimised (Figure 12b). This is distinct from the use of MVK+MACR ratios used by Xiong *et al.* where the purpose was to~~

620 ~~minimise the impact of uncertainties in the rates of physical processes.(Xiong et al., 2015) The $\Sigma C_4H_7NO_5$/(MVK+MACR) diurnals only slightly vary between each model. While the $\Sigma C_4H_7NO_5$/(MVK+MACR) in the models generally matches the measured ratio well, they show slightly stronger diurnal variation than is observed in the measurement, where the ratio remains relatively constant throughout the day. The time series for measured and modelled $\Sigma C_4H_7NO_5$ and $\Sigma C_4H_7NO_5$/(MVK+MACR) is given in Figure S13 and Figure S14.~~

625 ~~The results indicate that the formation of $C_4H_7NO_5$ from MVK and MACR, primarily through OH reaction pathways, is reasonably well represented in existing chemical mechanisms.~~

$\Sigma C_4H_7NO_5$ mixing ratios are under-predicted by around an order of magnitude in all models (Figure 13). The modelled $\Sigma C_4H_7NO_5$ diurnals only slightly vary between each model, despite the additional dark formation rates added to the FZJ mechanism, with the Caltech mechanism actually producing the highest concentrations. This is because the formation of

630 $\Sigma C_4H_7NO_5$ is dominated by the OH oxidation of MVK and MACR. The time series for measured and modelled $\Sigma C_4H_7NO_5$ is given in Figure S15.

The under-prediction in MVK+MACR and the potentially high ventilation (see Section 3.1) may account for some of this under-prediction, particularly in light of the potentially long lifetime of $C_4H_7NO_5$, however the under-prediction is much stronger than is observed for the MVK+MACR precursors. (Müller et al., 2014) Without previous work investigating the

635 sensitivity of I⁻-CIMS to $C_4H_7NO_5$ it is difficult to assess the impact of calibration on this measurement. Assuming a similar sensitivity as the most sensitively detected IHN isomer, where the OH and NO_3 groups are in close proximity like in the $C_4H_7NO_5$ isomers, would bring the measurement in line with the models.

4 Conclusions

Model results have been presented making use of three different detailed chemical mechanisms, comparing their predictions of several isoprene organonitrates. While the gas-phase box-modelling approach used here allows for the use of such complex mechanisms, the simplified representation may not fully represent physical processes such as boundary layer mixing in the morning and evening. Additionally, hydrolysis and aerosol uptake processes are not included in the mechanisms, meaning there may be unaccounted losses for species such as INHE. ~~Additionally, the measurement techniques potentially have significant issues with calibration factors, which can change over the course of a day as isomer composition changes. The~~While the impact of I⁻-CIMS sensitivity on measurements of these nitrates has been considered throughout this work, the availability of authentic standards would greatly improve the ability to quantify such organonitrates.

When considering ΣIPN, the model results presented here indicate that large proportions of the measured ΣIPN can be composed of non-IPN species. This is especially true during the ~~daytime~~day-time, when ΣIPN concentrations are lowest. However, the epoxide-forming reactions proposed by Vereecken *et al.* suggest that around half of the measured night-time ΣIPN could be comprised of INHE.(Vereecken et al., 2021) Assuming reactive uptake coefficients similar to those previously measured for IEPOX results in small reductions in predicted ΣIPN, ~~indicating~~meaning that ~~reactive uptake of INHE cannot fully explain the over prediction of ΣIPN made when using the~~ the FZJ mechanism predicts ΣIPN to be comprised of mostly non-IPN species for the majority of the day. Further studies of isoprene nitrate chemistry should investigate these species with techniques able to distinguish between the isomeric ΣIPN compounds and their reaction products, such as chromatographic techniques, in order to determine the role of INHE in isoprene oxidation. Such large INHE production terms would have implications for the formation and growth of secondary organic aerosol (SOA) by reactive uptake to acidified particles.(Hamilton et al., 2021) Generally, the large contribution of non-IPN species to the modelled ΣIPN highlights the caution that should be applied in interpreting measurements of ΣIPN solely as a measurement of IPN.

The changing distribution of ΣIHN isomers over the course of 24-hours has implications for the calibration of ΣIHN measurements. For example, I⁻-CIMS ~~will~~could be 2.5 to 1.4 times less sensitive to ~~IHN~~ΣIHN overnight where NO₃ chemistry is dominant, due to the increased contribution of E-1,4-IHN and E-4,1-IHN to ΣIHN. This means that the use of a constant calibration factor is likely to under-quantify night-time IHN, even if the calibration factor was accurate during the day. Furthermore, while comparison of the models to IEPOX-calibrated data suggests an under-prediction by the models, adjusting this calibration to account for the sensitivity of IHN isomers suggests a potentially very large over-prediction by the models.

The much improved ΣICN predictions when using the Caltech and FZJ Mechanisms compared to the MCM indicates that the assumptions around alkoxy radical decomposition made by the MCM are likely to be inaccurate~~.~~, even when calibration uncertainties are accounted for. Future studies focussed on isoprene nitrates should not overlook the inclusion of more complex INO decomposition routes, beyond the direct decomposition route to ICN present in the MCM.

17

~~When considering~~While the results presented here surrounding $C_4H_7NO_5$ ~~species,~~are not conclusive, there is potential for all of the mechanisms ~~reproduce $\Sigma C_4H_7NO_5$/(MVK+MACR) well, indicating the good representation of~~to be under-predicting $C_4H_7NO_5$ ~~chemistry, at least when the majority of the formation is resulting from MVK and MACR~~. Additional $C_4H_7NO_5$ from NO_3 chemistry, as is included in the FZJ Mechanism model, does not improve predictions as the majority of the modelled $C_4H_7NO_5$ resulted from OH chemistry. Assuming an I⁻-CIMS sensitivity of $C_4H_7NO_5$ similar to that of the more sensitively detected IHN isomers would mean that the modelled $C_4H_7NO_5$ is approximately correct.

~~The models generally predicted the concentrations of the four groups of isoprene derived organic nitrates well, and the improvements made by the inclusion of updated nitrate chemistry highlights the advances in the understanding of isoprene nitrate chemistry made in recent years. However, the work presented here illustrates some important remaining uncertainties surrounding the prediction of night-time concentrations of IPN, ICN, and IHN.~~

While physical processes dominated the loss of the organonitrates in all of the models presented here, the chemical losses of these species are not well understood. Estimated rate constants for the reaction of IHN, IPN, and ICN from Wennberg *et al.* indicate that the OH reactions which are included in all of the mechanisms may be the major chemical loss pathways, with NO_3 oxidation comprising a larger loss than reaction with O_3. This has implications for NO_x recycling, indicating that most of the NO_x consumed to form the organonitrates is subsequently lost from the gas-phase or transported away from the site of formation. (Bates and Jacob, 2019)

Generally, the mechanisms presented here do a reasonable job at reproducing isoprene nitrate chemistry in Beijing, particularly with the inclusion of improved alkoxy radical chemistry, though it is clear that better constraints on the sensitivity of I⁻-CIMS to nitrated compounds would aid in the analysis of these compounds.

Author Contributions

A.W.M performed the model simulations and prepared the manuscript. P.M.E and J.F.H provided supervision and advice throughout the project. B.H.L and J.A.T provided advice and feedback on the representation of isoprene nitrates in box-models and their measurement. A.R.R and B.S.N assisted in constructing the modelling approach and advised on the use of chemical mechanisms. T.J.B, J.B, J.R.H, J.D.L, C.P, and M.D.S carried out the measurements of species used for model constraints. All authors provided feedback on early drafts of the manuscript.

Competing interests

The authors declare that they have no conflict of interest.

Acknowledgements

Financial Support

References

Ayres, B. R., Allen, H. M., Draper, D. C., Brown, S. S., Wild, R. J., Jimenez, J. L., Day, D. A., Campuzano-Jost, P., Hu, W., de Gouw, J., Koss, A., Cohen, R. C., Duffey, K. C., Romer, P., Baumann, K., Edgerton, E., Takahama, S., Thornton, J. A., Lee, B. H., Lopez-Hilfiker, F. D., Mohr, C., Wennberg, P. O., Nguyen, T. B., Teng, A., Goldstein, A. H., Olson, K., and Fry, J. L.: Organic nitrate aerosol formation via NO3 + biogenic volatile organic compounds in the southeastern United States, Atmospheric Chemistry and Physics, 15, 13377-13392, 10.5194/acp-15-13377-2015, 2015.

Bates, K. H. and Jacob, D. J.: A new model mechanism for atmospheric oxidation of isoprene: global effects on oxidants, nitrogen oxides, organic products, and secondary organic aerosol, Atmospheric Chemistry and Physics, 19, 9613-9640, 10.5194/acp-19-9613-2019, 2019.

Brownwood, B., Turdziladze, A., Hohaus, T., Wu, R., Mentel, T. F., Carlsson, P. T. M., Tsiligiannis, E., Hallquist, M., Andres, S., Hantschke, L., Reimer, D., Rohrer, F., Tillmann, R., Winter, B., Liebmann, J., Brown, S. S., Kiendler-Scharr, A., Novelli, A., Fuchs, H., and Fry, J. L.: Gas-Particle Partitioning and SOA Yields of Organonitrate Products from NO3-Initiated Oxidation of Isoprene under Varied Chemical Regimes, ACS Earth Space Chem, 5, 785-800, 10.1021/acsearthspacechem.0c00311, 2021.

Budisulistiorini, S. H., Nenes, A., Carlton, A. G., Surratt, J. D., McNeill, V. F., and Pye, H. O. T.: Simulating Aqueous-Phase Isoprene-Epoxydiol (IEPOX) Secondary Organic Aerosol Production During the 2013 Southern Oxidant and Aerosol Study (SOAS), Environmental Science & Technology, 51, 5026-5034, 10.1021/acs.est.6b05750, 2017.

Chen, X., Wang, H., and Lu, K.: Simulation of organic nitrates in Pearl River Delta in 2006 and the chemical impact on ozone production, Science China Earth Sciences, 61, 228-238, 10.1007/s11430-017-9115-5, 2018.

Dunmore, R. E., Hopkins, J. R., Lidster, R. T., Lee, J. D., Evans, M. J., Rickard, A. R., Lewis, A. C., and Hamilton, J. F.: Diesel-related hydrocarbons can dominate gas phase reactive carbon in megacities, Atmospheric Chemistry and Physics, 15, 9983-9996, 10.5194/acp-15-9983-2015, 2015.

Emmerson, K. L. and Evans, M. J.: Comparison of tropospheric gas-phase chemistry schemes for use within global models, Atmos. Chem. Phys, 9, 1831-1845, https://doi.org/10.5194/acp-9-1831-2009, 2009.

735   Gaston, C. J., Riedel, T. P., Zhang, Z., Gold, A., Surratt, J. D., and Thornton, J. A.: Reactive Uptake of an Isoprene-Derived Epoxydiol to Submicron Aerosol Particles, Environmental Science & Technology, 48, 11178-11186, 10.1021/es5034266, 2014.

Guenther, A., Karl, T., Harley, P., Wiedinmyer, C., Palmer, P. I., and Geron, C.: Estimates of global terrestrial isoprene emissions using MEGAN (Model of Emissions of Gases and Aerosols from Nature), Atmospheric

740   Chemistry and Physics, 6, 3181-3210, 2006.

Guenther, A., Hewitt, C. N., Erickson, D., Fall, R., Geron, C., Graedel, T., Harley, P., Klinger, L., Lerdau, M., McKay, W. A., Pierce, T., Scholes, B., Steinbrecher, R., Tallamraju, R., Taylor, J., and Zimmerman, P.: A global model of natural volatile organic compound emissions, Journal of Geophysical Research, 100, 10.1029/94jd02950, 1995.

Guenther, A. B., Jiang, X., Heald, C. L., Sakulyanontvittaya, T., Duhl, T., Emmons, L. K., and Wang, X.: The Model

745   of Emissions of Gases and Aerosols from Nature version 2.1 (MEGAN2.1): an extended and updated framework for modeling biogenic emissions, Geoscientific Model Development, 5, 1471-1492, 10.5194/gmd-5-1471-2012, 2012.

Hamilton, J. F., Bryant, D. J., Edwards, P. M., Ouyang, B., Bannan, T. J., Mehra, A., Mayhew, A. W., Hopkins, J. R., Dunmore, R. E., Squires, F. A., Lee, J. D., Newland, M. J., Worrall, S. D., Bacak, A., Coe, H., Percival, C., Whalley, L.

750   K., Heard, D. E., Slater, E. J., Jones, R. L., Cui, T., Surratt, J. D., Reeves, C. E., Mills, G. P., Grimmond, S., Sun, Y., Xu, W., Shi, Z., and Rickard, A. R.: Key Role of NO3 Radicals in the Production of Isoprene Nitrates and Nitrooxyorganosulfates in Beijing, Environ Sci Technol, 55, 842-853, 10.1021/acs.est.0c05689, 2021.

Hopkins, J. R., Jones, C. E., and Lewis, A. C.: A dual channel gas chromatograph for atmospheric analysis of volatile organic compounds including oxygenated and monoterpene compounds, J Environ Monit, 13, 2268-

755   2276, 10.1039/c1em10050e, 2011.

Huang, Z., Zhang, Y., Yan, Q., Zhang, Z., and Wang, X.: Real-time monitoring of respiratory absorption factors of volatile organic compounds in ambient air by proton transfer reaction time-of-flight mass spectrometry, J Hazard Mater, 320, 547-555, 10.1016/j.jhazmat.2016.08.064, 2016.

Iyer, S., Lopez-Hilfiker, F., Lee, B. H., Thornton, J. A., and Kurtén, T.: Modeling the Detection of Organic and

760   Inorganic Compounds Using Iodide-Based Chemical Ionization, The Journal of Physical Chemistry A, 120, 576-587, 10.1021/acs.jpca.5b09837, 2016.

Jenkin, M. E., Saunders, S. M., and Pilling, M. J.: The Tropospheric Degradation of Volatile Organic Compounds: A Protocol for Mechanism Development, Atmospheric Environment, 81-104, https://doi.org/10.1016/S1352-2310(96)00105-7, 1997.

765   Jenkin, M. E., Young, J. C., and Rickard, A. R.: The MCM v3.3.1 degradation scheme for isoprene, Atmospheric Chemistry and Physics, 15, 11433-11459, 10.5194/acp-15-11433-2015, 2015.

Lee, B. H., Lopez-Hilfiker, F. D., Mohr, C., Kurten, T., Worsnop, D. R., and Thornton, J. A.: An iodide-adduct high-resolution time-of-flight chemical-ionization mass spectrometer: application to atmospheric inorganic and organic compounds, Environ Sci Technol, 48, 6309-6317, 10.1021/es500362a, 2014.

770   Liu, S., Shilling, J. E., Song, C., Hiranuma, N., Zaveri, R. A., and Russell, L. M.: Hydrolysis of Organonitrate Functional Groups in Aerosol Particles, Aerosol Science and Technology, 46, 1359-1369, 10.1080/02786826.2012.716175, 2012.

Lopez-Hilfiker, F. D., Mohr, C., Ehn, M., Rubach, F., Kleist, E., Wildt, J., Mentel, T. F., Lutz, A., Hallquist, M., Worsnop, D., and Thornton, J. A.: A novel method for online analysis of gas and particle composition:

775 description and evaluation of a Filter Inlet for Gases and AEROsols (FIGAERO), Atmospheric Measurement Techniques, 7, 983-1001, 10.5194/amt-7-983-2014, 2014.

Mohr, C., Thornton, J. A., Heitto, A., Lopez-Hilfiker, F. D., Lutz, A., Riipinen, I., Hong, J., Donahue, N. M., Hallquist, M., Petäjä, T., Kulmala, M., and Yli-Juuti, T.: Molecular identification of organic vapors driving atmospheric nanoparticle growth, Nature Communications, 10, 10.1038/s41467-019-12473-2, 2019.

780 Müller, J. F., Peeters, J., and Stavrakou, T.: Fast photolysis of carbonyl nitrates from isoprene, Atmospheric Chemistry and Physics, 14, 2497-2508, 10.5194/acp-14-2497-2014, 2014.

Newland, M. J., Bryant, D. J., Dunmore, R. E., Bannan, T. J., Acton, W. J. F., Langford, B., Hopkins, J. R., Squires, F. A., Dixon, W., Drysdale, W. S., Ivatt, P. D., Evans, M. J., Edwards, P. M., Whalley, L. K., Heard, D. E., Slater, E. J., Woodward-Massey, R., Ye, C., Mehra, A., Worrall, S. D., Bacak, A., Coe, H., Percival, C. J., Hewitt, C. N., Lee, J. D.,
785 Cui, T., Surratt, J. D., Wang, X., Lewis, A. C., Rickard, A. R., and Hamilton, J. F.: Low-NO atmospheric oxidation pathways in a polluted megacity, Atmospheric Chemistry and Physics, 21, 1613-1625, 10.5194/acp-21-1613-2021, 2021.

Nguyen, T. B., Crounse, J. D., Teng, A. P., St. Clair, J. M., Paulot, F., Wolfe, G. M., and Wennberg, P. O.: Rapid deposition of oxidized biogenic compounds to a temperate forest, Proceedings of the National Academy of
790 Sciences, 112, E392-E401, 10.1073/pnas.1418702112, 2015.

Nguyen, T. B., Coggon, M. M., Bates, K. H., Zhang, X., Schwantes, R. H., Schilling, K. A., Loza, C. L., Flagan, R. C., Wennberg, P. O., and Seinfeld, J. H.: Organic aerosol formation from the reactive uptake of isoprene epoxydiols (IEPOX) onto non-acidified inorganic seeds, Atmospheric Chemistry and Physics, 14, 3497-3510, 10.5194/acp-14-3497-2014, 2014.

795 Novelli, A., Cho, C., Fuchs, H., Hofzumahaus, A., Rohrer, F., Tillmann, R., Kiendler-Scharr, A., Wahner, A., and Vereecken, L.: Experimental and theoretical study on the impact of a nitrate group on the chemistry of alkoxy radicals, Phys Chem Chem Phys, 23, 5474-5495, 10.1039/d0cp05555g, 2021.

Palmer, P. I., Marvin, M. R., Siddans, R., Kerridge, B. J., and Moore, D. P.: Nocturnal survival of isoprene linked to formation of upper tropospheric organic aerosol, Science, 375, 562-566, 10.1126/science.abg4506, 2022.

800 Paulot, F., Crounse, J. D., Kjaergaard, H. G., Kürten, A., St Clair, J. M., Seinfeld, J. H., and Wennberg, P. O.: Unexpected Epoxide Formation in the Gas-Phase Photooxidation of Isoprene, Science, 325, 730-733, 10.1126/science.1172910, 2009.

Praske, E., Crounse, J. D., Bates, K. H., Kurten, T., Kjaergaard, H. G., and Wennberg, P. O.: Atmospheric fate of methyl vinyl ketone: peroxy radical reactions with NO and HO2, J Phys Chem A, 119, 4562-4572,
805 10.1021/jp5107058, 2015.

Pratt, K. A., Mielke, L. H., Shepson, P. B., Bryan, A. M., Steiner, A. L., Ortega, J., Daly, R., Helmig, D., Vogel, C. S., Griffith, S., Dusanter, S., Stevens, P. S., and Alaghmand, M.: Contributions of individual reactive biogenic volatile organic compounds to organic nitrates above a mixed forest, Atmospheric Chemistry and Physics, 12, 10125-10143, 10.5194/acp-12-10125-2012, 2012.

810 Reeves, C. E., Mills, G. P., Whalley, L. K., Acton, W. J. F., Bloss, W. J., Crilley, L. R., Grimmond, S., Heard, D. E., Hewitt, C. N., Hopkins, J. R., Kotthaus, S., Kramer, L. J., Jones, R. L., Lee, J. D., Liu, Y., Ouyang, B., Slater, E., Squires, F., Wang, X., Woodward-Massey, R., and Ye, C.: Observations of speciated isoprene nitrates in Beijing: implications for isoprene chemistry, Atmospheric Chemistry and Physics, 21, 6315-6330, 10.5194/acp-21-6315-2021, 2021.

815 Riedel, T. P., Lin, Y. H., Zhang, Z., Chu, K., Thornton, J. A., Vizuete, W., Gold, A., and Surratt, J. D.: Constraining condensed-phase formation kinetics of secondary organic aerosol components from isoprene epoxydiols, Atmos. Chem. Phys, 16, 1245-1254, 10.5194/acpd-15-28289-2015, 2016.

Riedel, T. P., Lin, Y.-H., Budisulistiorini, S. H., Gaston, C. J., Thornton, J. A., Zhang, Z., Vizuete, W., Gold, A., and Surratt, J. D.: Heterogeneous Reactions of Isoprene-Derived Epoxides: Reaction Probabilities and Molar

820 Secondary Organic Aerosol Yield Estimates, Environmental Science & Technology Letters, 2, 38-42, 10.1021/ez500406f, 2015.

Rivera-Rios, J. C., Nguyen, T. B., Crounse, J. D., Jud, W., St. Clair, J. M., Mikoviny, T., Gilman, J. B., Lerner, B. M., Kaiser, J. B., Gouw, J., Wisthaler, A., Hansel, A., Wennberg, P. O., Seinfeld, J. H., and Keutsch, F. N.: Conversion of hydroperoxides to carbonyls in field and laboratory instrumentation: Observational bias in diagnosing pristine

825 versus anthropogenically controlled atmospheric chemistry, Geophysical Research Letters, 41, 8645-8651, 10.1002/2014gl061919, 2014.

Romer, P. S., Duffey, K. C., Wooldridge, P. J., Allen, H. M., Ayres, B. R., Brown, S. S., Brune, W. H., Crounse, J. D., De Gouw, J., Draper, D. C., Feiner, P. A., Fry, J. L., Goldstein, A. H., Koss, A., Misztal, P. K., Nguyen, T. B., Olson, K., Teng, A. P., Wennberg, P. O., Wild, R. J., Zhang, L., and Cohen, R. C.: The lifetime of nitrogen oxides in an

830 isoprene-dominated forest, Atmospheric Chemistry and Physics, 16, 7623-7637, 10.5194/acp-16-7623-2016, 2016.

Schwantes, R. H., Charan, S. M., Bates, K. H., Huang, Y., Nguyen, T. B., Mai, H., Kong, W., Flagan, R. C., and Seinfeld, J. H.: Low-volatility compounds contribute significantly to isoprene secondary organic aerosol (SOA) under high-NOx conditions, Atmospheric Chemistry and Physics, 19, 7255-7278, 10.5194/acp-19-7255-2019,

835 2019.

Schwantes, R. H., Teng, A. P., Nguyen, T. B., Coggon, M. M., Crounse, J. D., St. Clair, J. M., Zhang, X., Schilling, K. A., Seinfeld, J. H., and Wennberg, P. O.: Isoprene NO3 Oxidation Products from the RO2 + HO2 Pathway, Journal of Physical Chemistry A, 119, 10158-10171, 10.1021/acs.jpca.5b06355, 2015.

Schwantes, R. H., Emmons, L. K., Orlando, J. J., Barth, M. C., Tyndall, G. S., Hall, S. R., Ullmann, K., St. Clair, J. M.,

840 Blake, D. R., Wisthaler, A., and Bui, T. P. V.: Comprehensive isoprene and terpene gas-phase chemistry improves simulated surface ozone in the southeastern US, Atmospheric Chemistry and Physics, 20, 3739-3776, 10.5194/acp-20-3739-2020, 2020.

Shi, Z., Vu, T., Kotthaus, S., Harrison, R. M., Grimmond, S., Yue, S., Zhu, T., Lee, J., Han, Y., Demuzere, M., Dunmore, R. E., Ren, L., Liu, D., Wang, Y., Wild, O., Allan, J., Acton, W. J., Barlow, J., Barratt, B., Beddows, D.,

845 Bloss, W. J., Calzolai, G., Carruthers, D., Carslaw, D. C., Chan, Q., Chatzidiakou, L., Chen, Y., Crilley, L., Coe, H., Dai, T., Doherty, R., Duan, F., Fu, P., Ge, B., Ge, M., Guan, D., Hamilton, J. F., He, K., Heal, M., Heard, D., Hewitt, C. N., Hollaway, M., Hu, M., Ji, D., Jiang, X., Jones, R., Kalberer, M., Kelly, F. J., Kramer, L., Langford, B., Lin, C., Lewis, A. C., Li, J., Li, W., Liu, H., Liu, J., Loh, M., Lu, K., Lucarelli, F., Mann, G., McFiggans, G., Miller, M. R., Mills, G., Monk, P., Nemitz, E., O'Connor, F., Ouyang, B., Palmer, P. I., Percival, C., Popoola, O., Reeves, C., Rickard, A.

850 R., Shao, L., Shi, G., Spracklen, D., Stevenson, D., Sun, Y., Sun, Z., Tao, S., Tong, S., Wang, Q., Wang, W., Wang, X., Wang, X., Wang, Z., Wei, L., Whalley, L., Wu, X., Wu, Z., Xie, P., Yang, F., Zhang, Q., Zhang, Y., Zhang, Y., and Zheng, M.: Introduction to the special issue "In-depth study of air pollution sources and processes within Beijing and its surrounding region (APHH-Beijing)", Atmospheric Chemistry and Physics, 19, 7519-7546, 10.5194/acp-19-7519-2019, 2019.

855 Sindelarova, K., Granier, C., Bouarar, I., Guenther, A., Tilmes, S., Stavrakou, T., Müller, J. F., Kuhn, U., Stefani, P., and Knorr, W.: Global data set of biogenic VOC emissions calculated by the MEGAN model over the last 30 years, Atmospheric Chemistry and Physics, 14, 9317-9341, 10.5194/acp-14-9317-2014, 2014.

Sommariva, R., Cox, S., Martin, C., Borońska, K., Young, J., Jimack, P., Pilling, M. J., Matthaios, V. N., Newland, M. J., Panagi, M., Bloss, W. J., Monks, P. S., and Rickard, A. R.: AtChem, an open source box-model for the Master

860 Chemical Mechanism, Geoscientific Model Development, 10.5194/gmd-2019-192, 2019.

Surratt, J. D., Chan, A. W. H., Eddingsaas, N. C., Chan, M., Loza, C. L., Kwan, A. J., Hersey, S. P., Flagan, R. C., Wennberg, P. O., and Seinfeld, J. H.: Reactive intermediates revealed in secondary organic aerosol formation from isoprene, Proceedings of the National Academy of Sciences, 107, 6640-6645, 10.1073/pnas.0911114107, 2010.

865 Tsiligiannis, E., Wu, R., Lee, B. H., ~~Garcia~~ Salvador, C. M., Priestley, M., Carlsson, P. T. M., Kang, S., Novelli, A., Vereecken, L., Fuchs, H., Mayhew, A. W., Hamilton, J. F., Edwards, P. M., Fry, J. L., Brownwood, B., Brown, S. S., Wild, R. J., Bannan, T. J., Coe, H., Allan, J., Surratt, J. D., Bacak, A., Artaxo, P., Percival, C., Guo, S., Hu, M., Wang, T., Mentel, T. F., Thornton, J. A., and Hallquist, M.: A ~~four carbon organonitrate~~ Four Carbon Organonitrate as a ~~significant product~~ Significant Product of ~~secondary isoprene chemistry, Geophys. Res. Lett.,~~ Secondary Isoprene

870 Chemistry, Geophysical Research Letters, 49, 10.1029/2021gl097366, 2022 ~~(under review).~~.

Vasquez, K. T., Crounse, J. D., Schulze, B. C., Bates, K. H., Teng, A. P., Xu, L., Allen, H. M., and Wennberg, P. O.: Rapid hydrolysis of tertiary isoprene nitrate efficiently removes NOx from the atmosphere, Proc Natl Acad Sci U S A, 117, 33011-33016, 10.1073/pnas.2017442117, 2020.

Vereecken, L., Carlsson, P. T. M., Novelli, A., Bernard, F., Brown, S. S., Cho, C., Crowley, J. N., Fuchs, H., Mellouki,
875 W., Reimer, D., Shenolikar, J., Tillmann, R., Zhou, L., Kiendler-Scharr, A., and Wahner, A.: Theoretical and experimental study of peroxy and alkoxy radicals in the NO3-initiated oxidation of isoprene, Phys Chem Chem Phys, 23, 5496-5515, 10.1039/d0cp06267g, 2021.

Wennberg, P. O., Bates, K. H., Crounse, J. D., Dodson, L. G., McVay, R. C., Mertens, L. A., Nguyen, T. B., Praske, E., Schwantes, R. H., Smarte, M. D., St Clair, J. M., Teng, A. P., Zhang, X., and Seinfeld, J. H.: Gas-Phase Reactions
880 of Isoprene and Its Major Oxidation Products, Chemical Reviews, 118, 3337-3390, 10.1021/acs.chemrev.7b00439, 2018.

Whalley, L. K., Stone, D., Dunmore, R., Hamilton, J., Hopkins, J. R., Lee, J. D., Lewis, A. C., Williams, P., Kleffmann, J., Laufs, S., Woodward-Massey, R., and Heard, D. E.: Understanding in situ ozone production in the summertime through radical observations and modelling studies during the Clean air for London project
885 (ClearfLo), Atmospheric Chemistry and Physics, 18, 2547-2571, 10.5194/acp-18-2547-2018, 2018.

Whalley, L. K., Furneaux, K. L., Goddard, A., Lee, J. D., Mahajan, A., Oetjen, H., Read, K. A., Kaaden, N., Carpenter, L. J., Lewis, A. C., Plane, J. M. C., Saltzman, E. S., Wiedensohler, A., and Heard, D. E.: The chemistry of OH and HO2 radicals in the boundary layer over the tropical Atlantic Ocean, Atmospheric Chemistry and Physics, 10, 1555-1576, 10.5194/acp-10-1555-2010, 2010.

890 Whalley, L. K., Slater, E. J., Woodward-Massey, R., Ye, C., Lee, J. D., Squires, F., Hopkins, J. R., Dunmore, R. E., Shaw, M., Hamilton, J. F., Lewis, A. C., Mehra, A., Worrall, S. D., Bacak, A., Bannan, T. J., Coe, H., Percival, C. J., Ouyang, B., Jones, R. L., Crilley, L. R., Kramer, L. J., Bloss, W. J., Vu, T., Kotthaus, S., Grimmond, S., Sun, Y., Xu, W., Yue, S., Ren, L., Acton, W. J. F., Hewitt, C. N., Wang, X., Fu, P., and Heard, D. E.: Evaluating the sensitivity of radical chemistry and ozone formation to ambient VOCs and NOx in Beijing, Atmospheric Chemistry and Physics,
895 21, 2125-2147, 10.5194/acp-21-2125-2021, 2021.

Wu, R., Vereecken, L., Tsiligiannis, E., Kang, S., Albrecht, S. R., Hantschke, L., Zhao, D., Novelli, A., Fuchs, H., Tillmann, R., Hohaus, T., Carlsson, P. T. M., Shenolikar, J., Bernard, F., Crowley, J. N., Fry, J. L., Brownwood, B., Thornton, J. A., Brown, S. S., Kiendler-Scharr, A., Wahner, A., Hallquist, M., and Mentel, T. F.: Molecular composition and volatility of multi-generation products formed from isoprene oxidation by nitrate radical,
900 Atmospheric Chemistry and Physics, 21, 10799-10824, 10.5194/acp-21-10799-2021, 2021.

Xiong, F., McAvey, K. M., Pratt, K. A., Groff, C. J., Hostetler, M. A., Lipton, M. A., Starn, T. K., Seeley, J. V., Bertman, S. B., Teng, A. P., Crounse, J. D., Nguyen, T. B., Wennberg, P. O., Misztal, P. K., Goldstein, A. H., Guenther, A. B., Koss, A. R., Olson, K. F., De Gouw, J. A., Baumann, K., Edgerton, E. S., Feiner, P. A., Zhang, L.,

Miller, D. O., Brune, W. H., and Shepson, P. B.: Observation of isoprene hydroxynitrates in the southeastern United States and implications for the fate of NOx, Atmospheric Chemistry and Physics, 15, 11257-11272, 10.5194/acp-15-11257-2015, 2015.

Zare, A., Romer, P. S., Nguyen, T., Keutsch, F. N., Skog, K., and Cohen, R. C.: A comprehensive organic nitrate chemistry: insights into the lifetime of atmospheric organic nitrates, Atmospheric Chemistry and Physics, 18, 15419-15436, 10.5194/acp-18-15419-2018, 2018.

Zaveri, R. A., Shilling, J. E., Fast, J. D., and Springston, S. R.: Efficient Nighttime Biogenic SOA Formation in a Polluted Residual Layer, Journal of Geophysical Research: Atmospheres, 10.1029/2019jd031583, 2020.

Zhou, W., Zhao, J., Ouyang, B., Mehra, A., Xu, W., Wang, Y., Bannan, T. J., Worrall, S. D., Priestley, M., Bacak, A., Chen, Q., Xie, C., Wang, Q., Wang, J., Du, W., Zhang, Y., Ge, X., Ye, P., Lee, J. D., Fu, P., Wang, Z., Worsnop, D., Jones, R., Percival, C. J., Coe, H., and Sun, Y.: Production of N2O5 and ClNO2 in summer in urban Beijing, China, Atmospheric Chemistry and Physics, 18, 11581-11597, 10.5194/acp-18-11581-2018, 2018.
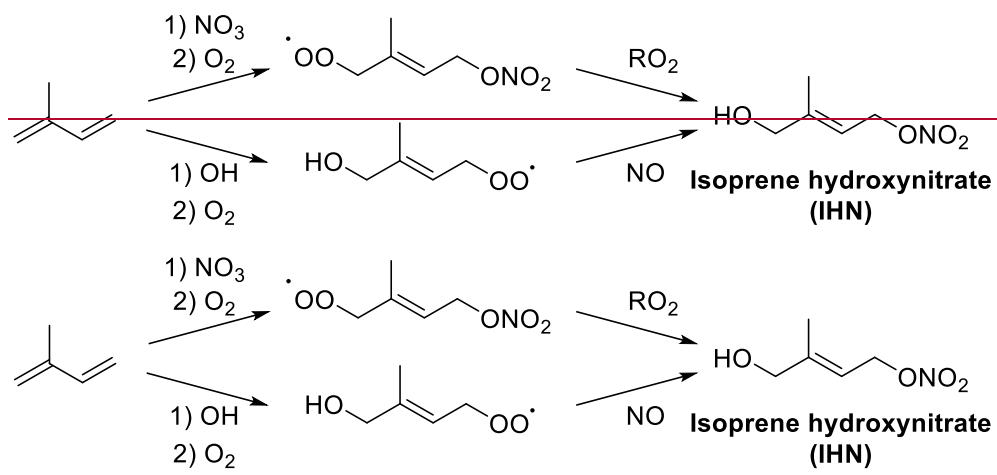
Figure 1. OH-initiated and NO₃-initiated formation of IHN. The formation of 1,4-IHN is shown here, other IHN isomers, as well as additional reaction products, will also be formed.
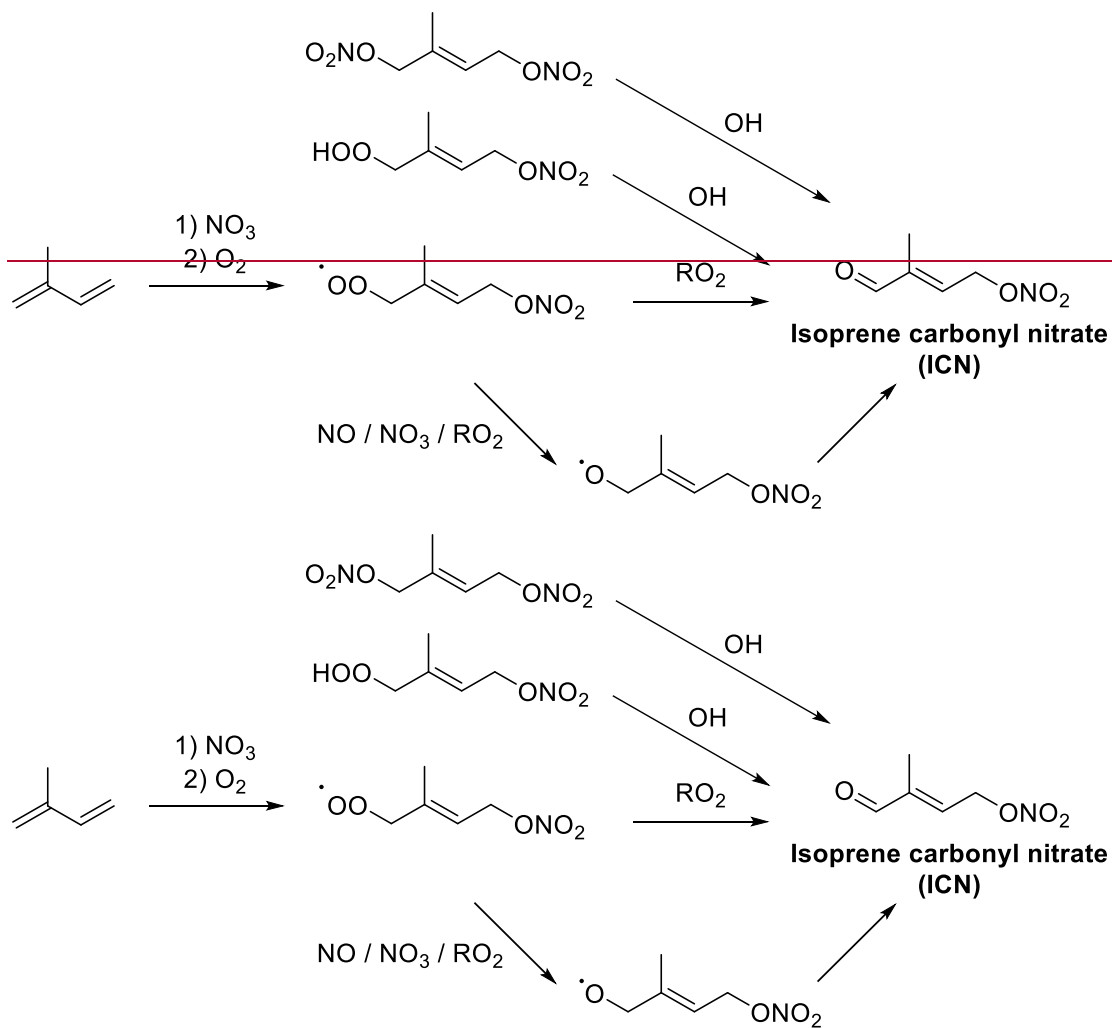
Figure 2. NO$_3$-initiated formation of ICN. The formation of 1,4-ICN is shown here, other ICN isomers, as well as additional reaction products, will also be formed.

25
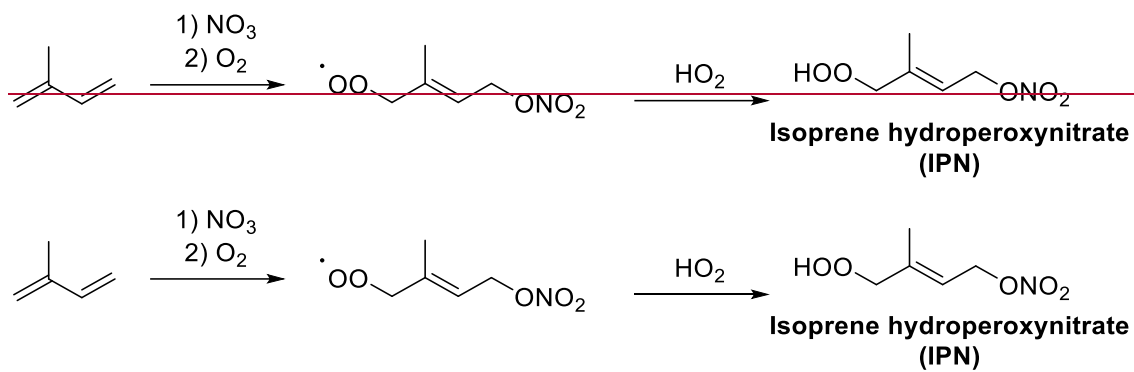
Figure 3. NO₃-initiated formation of IPN. The formation of 1,4-IPN is shown here, other IPN isomers, as well as additional reaction products, will also be formed.
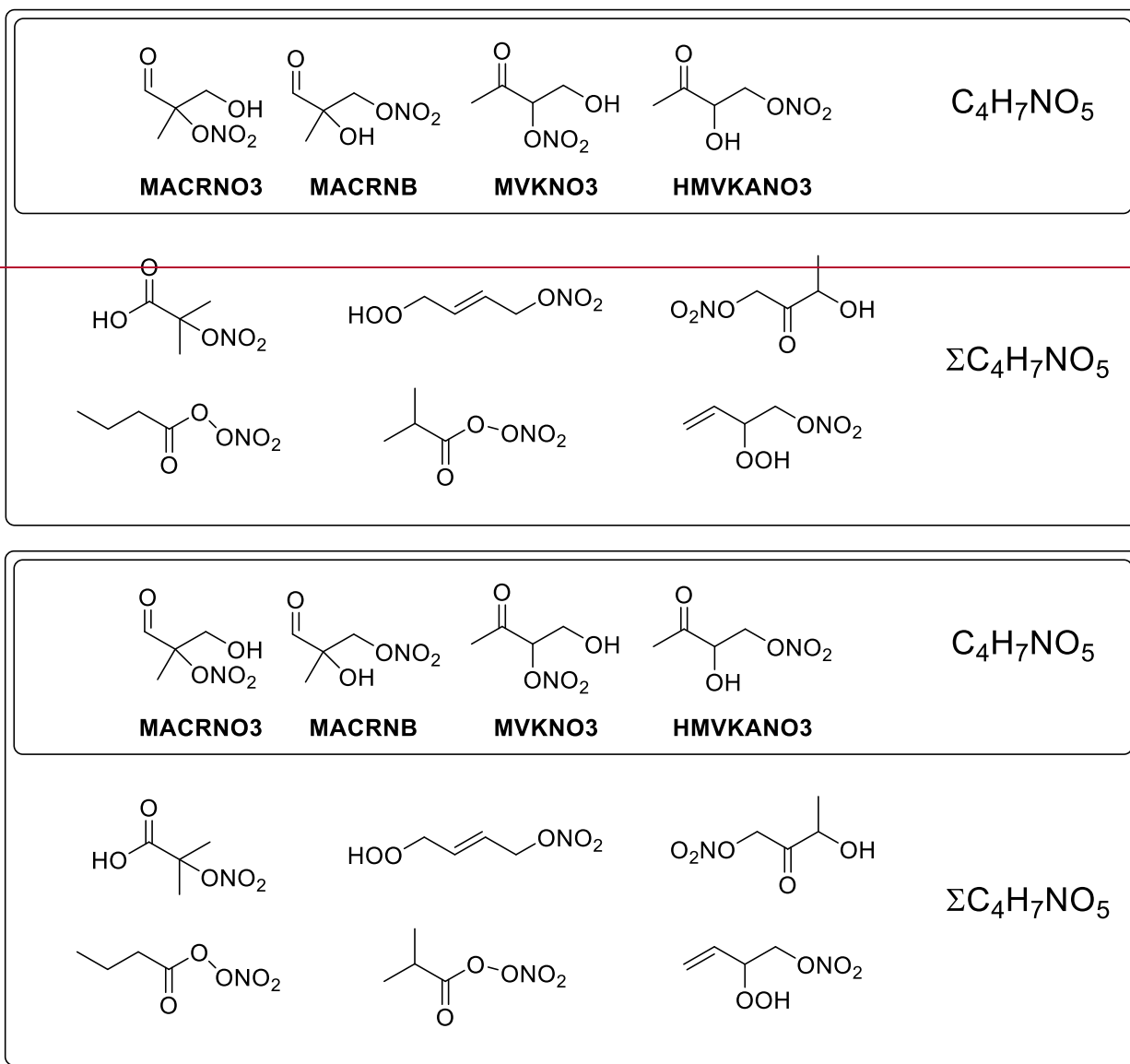
Figure 4. The four C₄H₇NO₅ species resulting from isoprene oxidation present in the MCM along with the additional isomeric compounds which complete the set of ΣC₄H₇NO₅
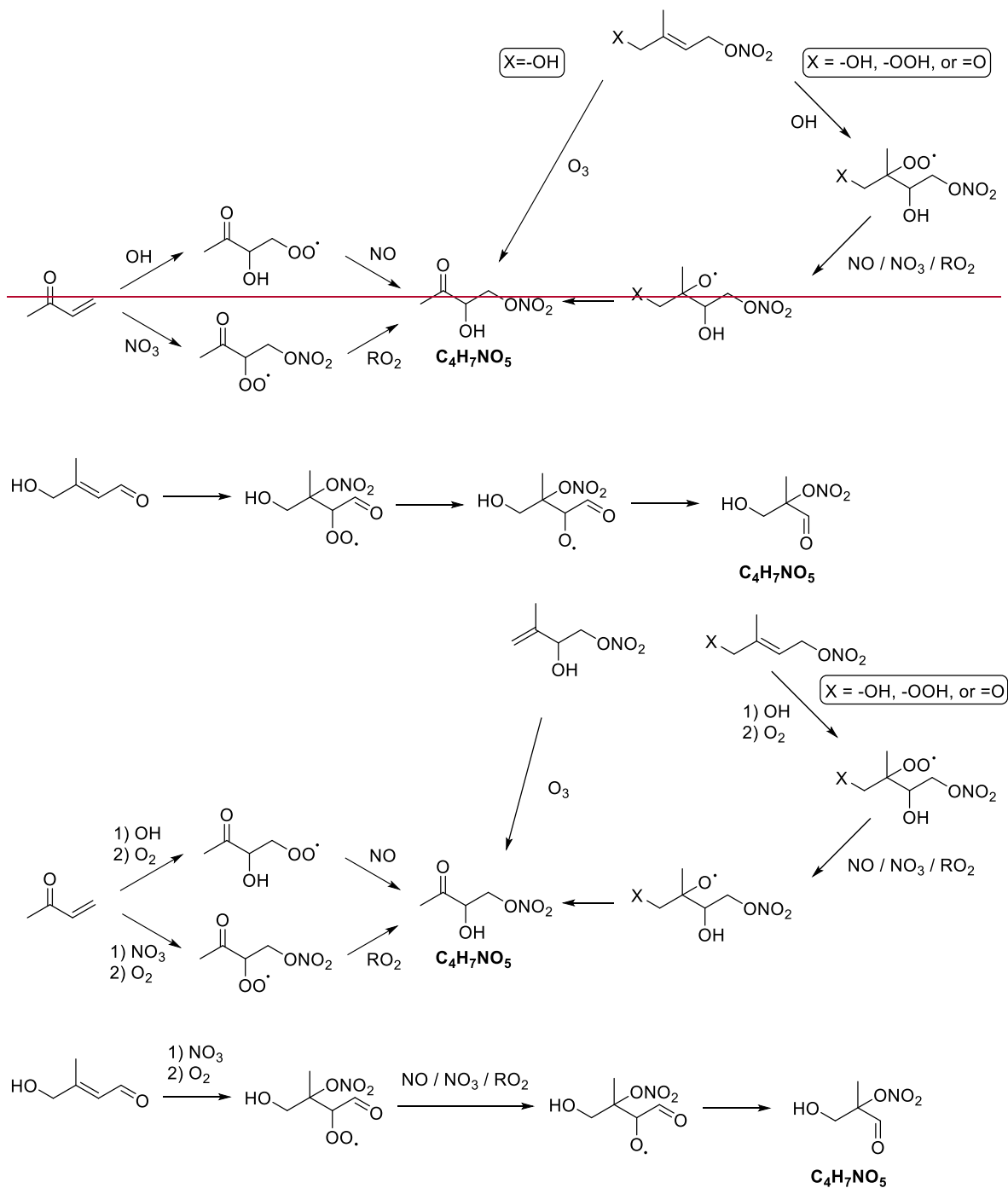
Figure 5. Formation of C₄H₇NO₅ compounds. Only two isomers are shown here, other formation routes for these and other isomers are also present. Additional reaction products will also be formed.
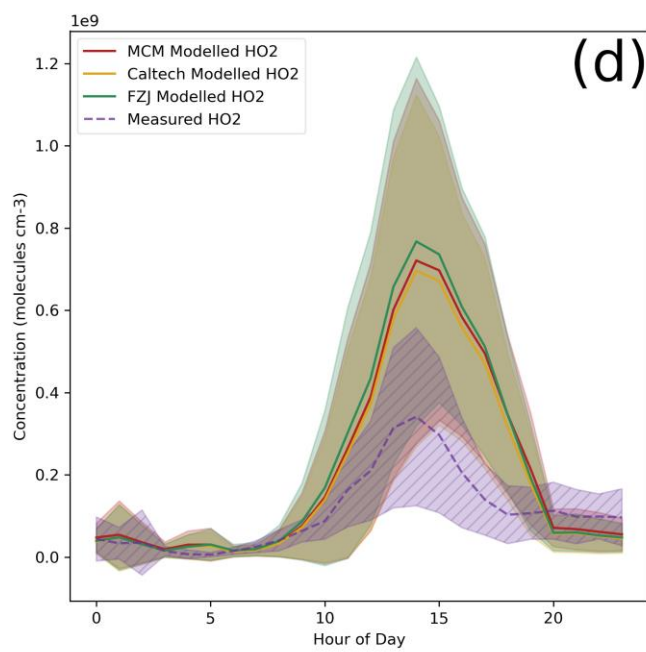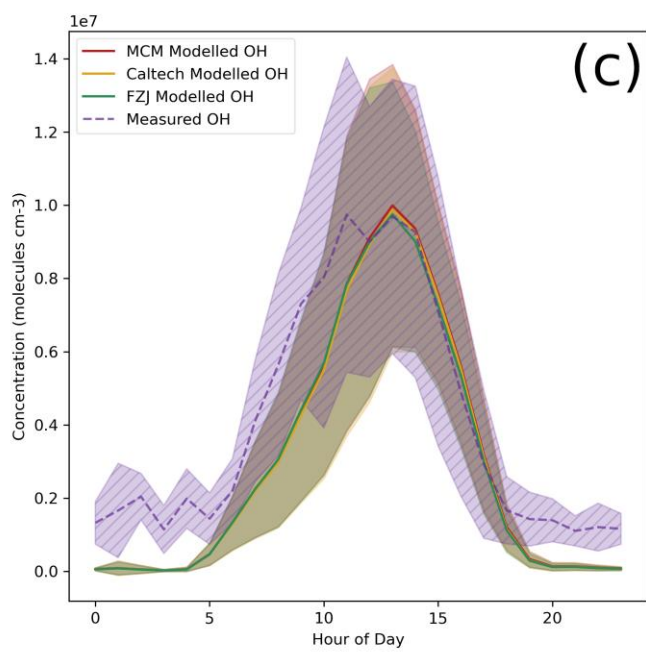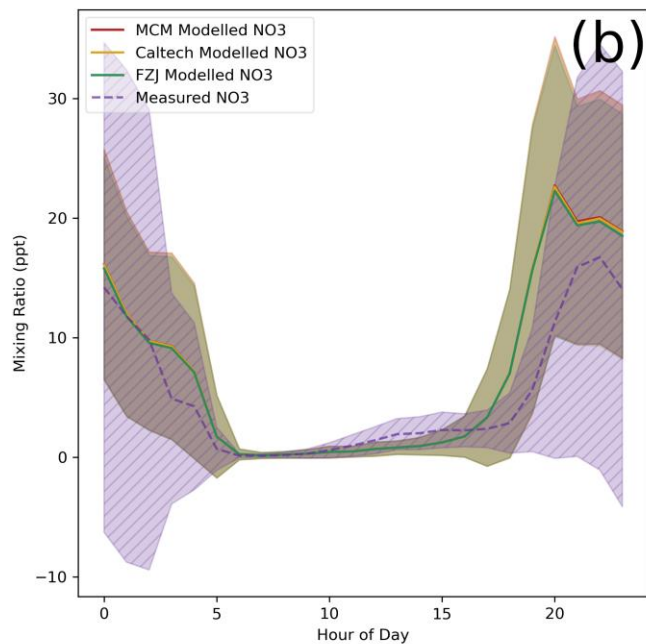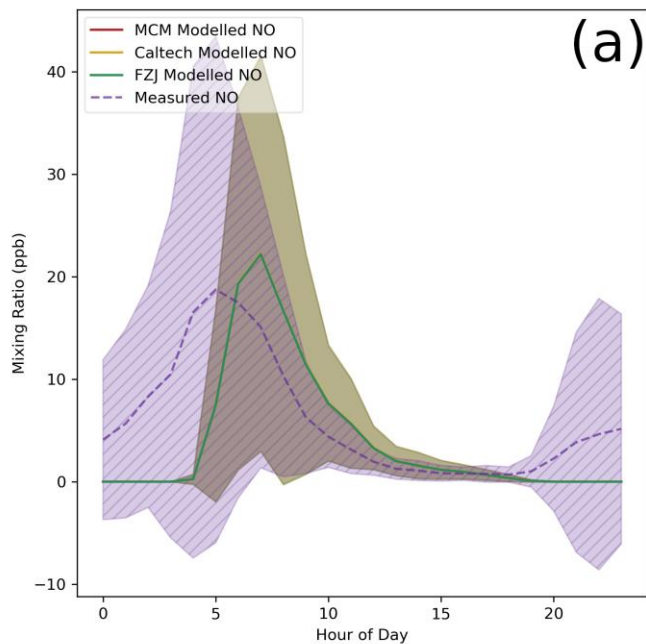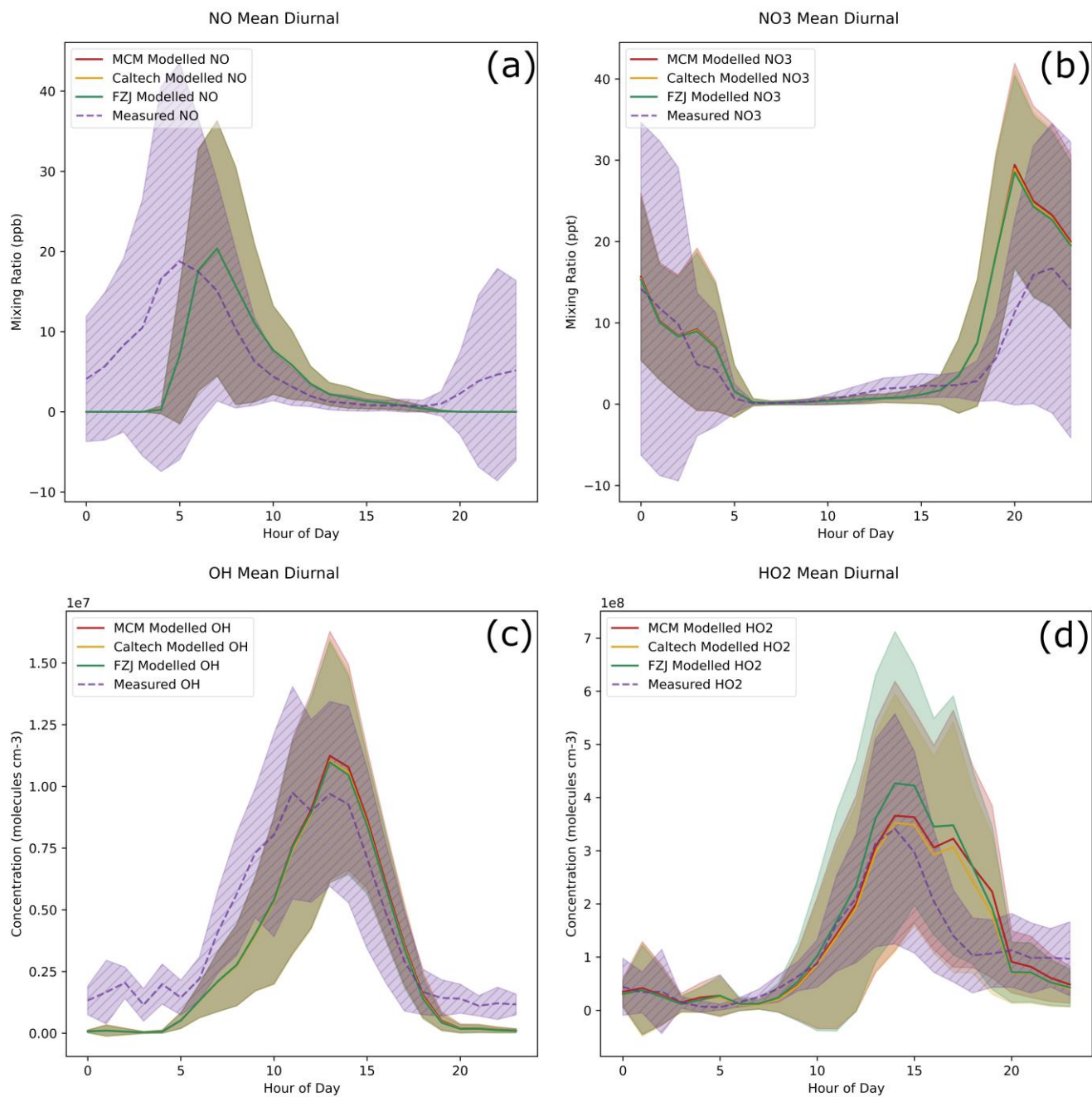
Figure 6. A selection measured values and model predictions of inorganic species left unconstrained in the models. Each line shows the mean value for each dataset, with the shaded area indicating one standard deviation above and below the mean. The values of NO from each model are all overlapping in (a).
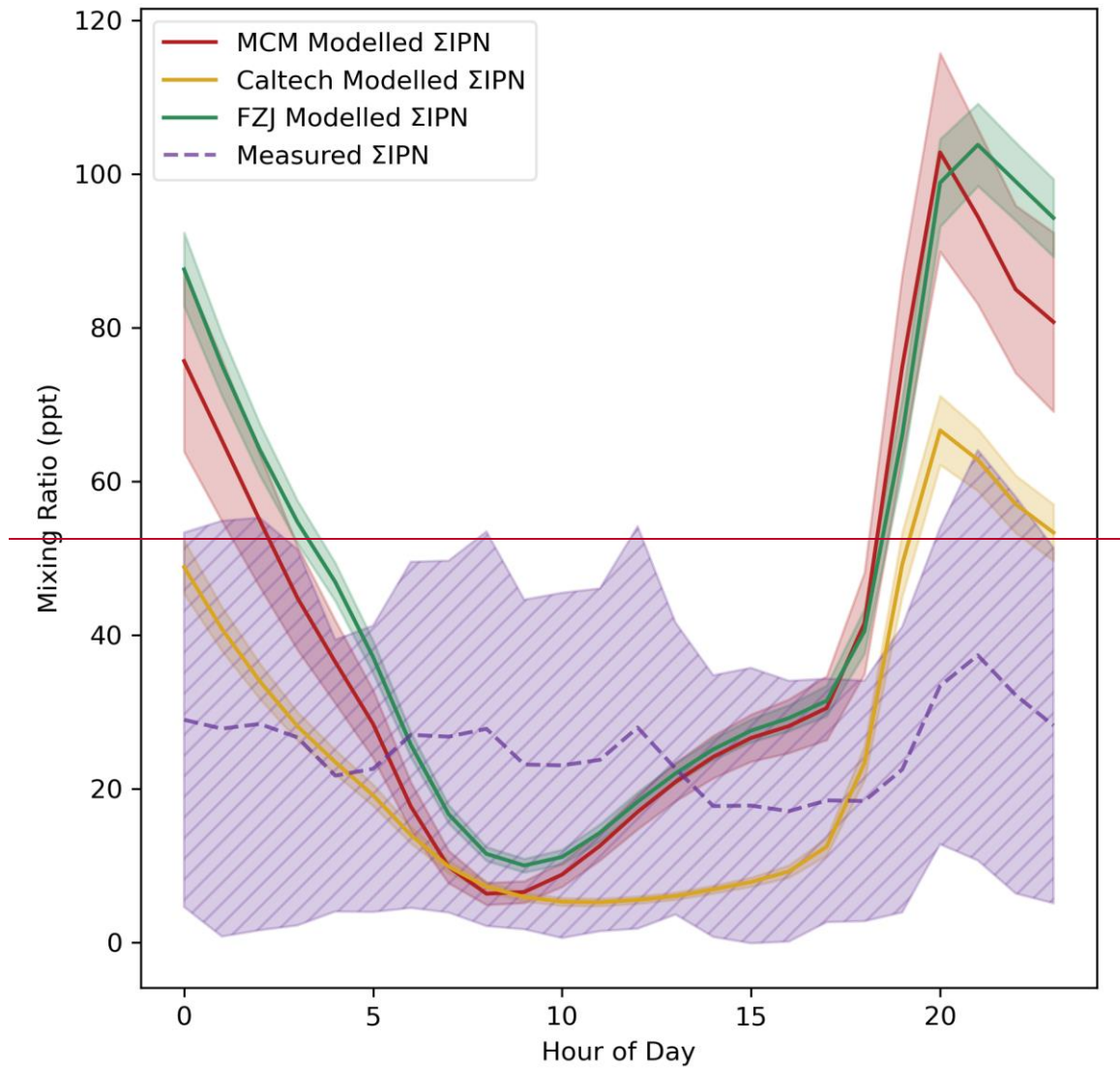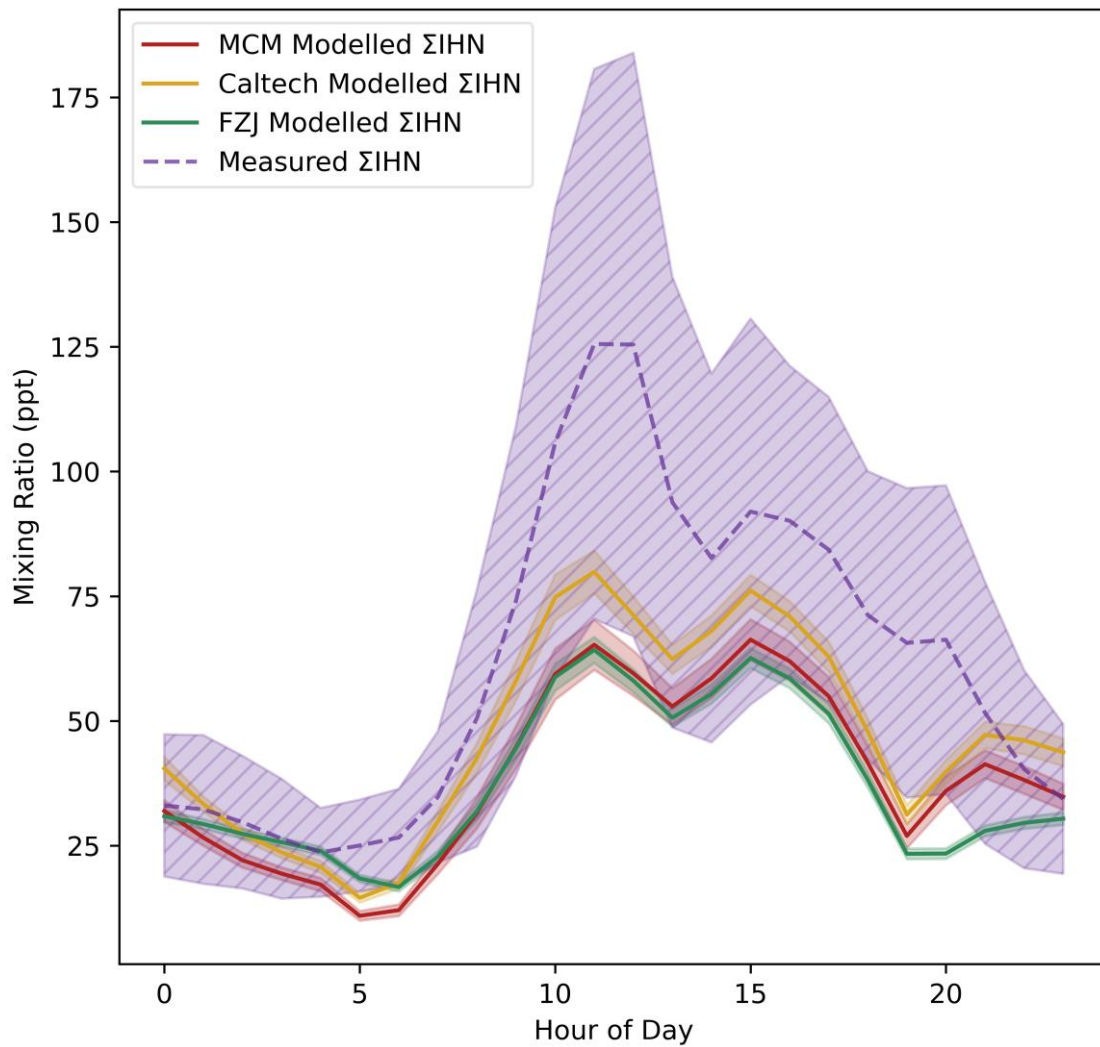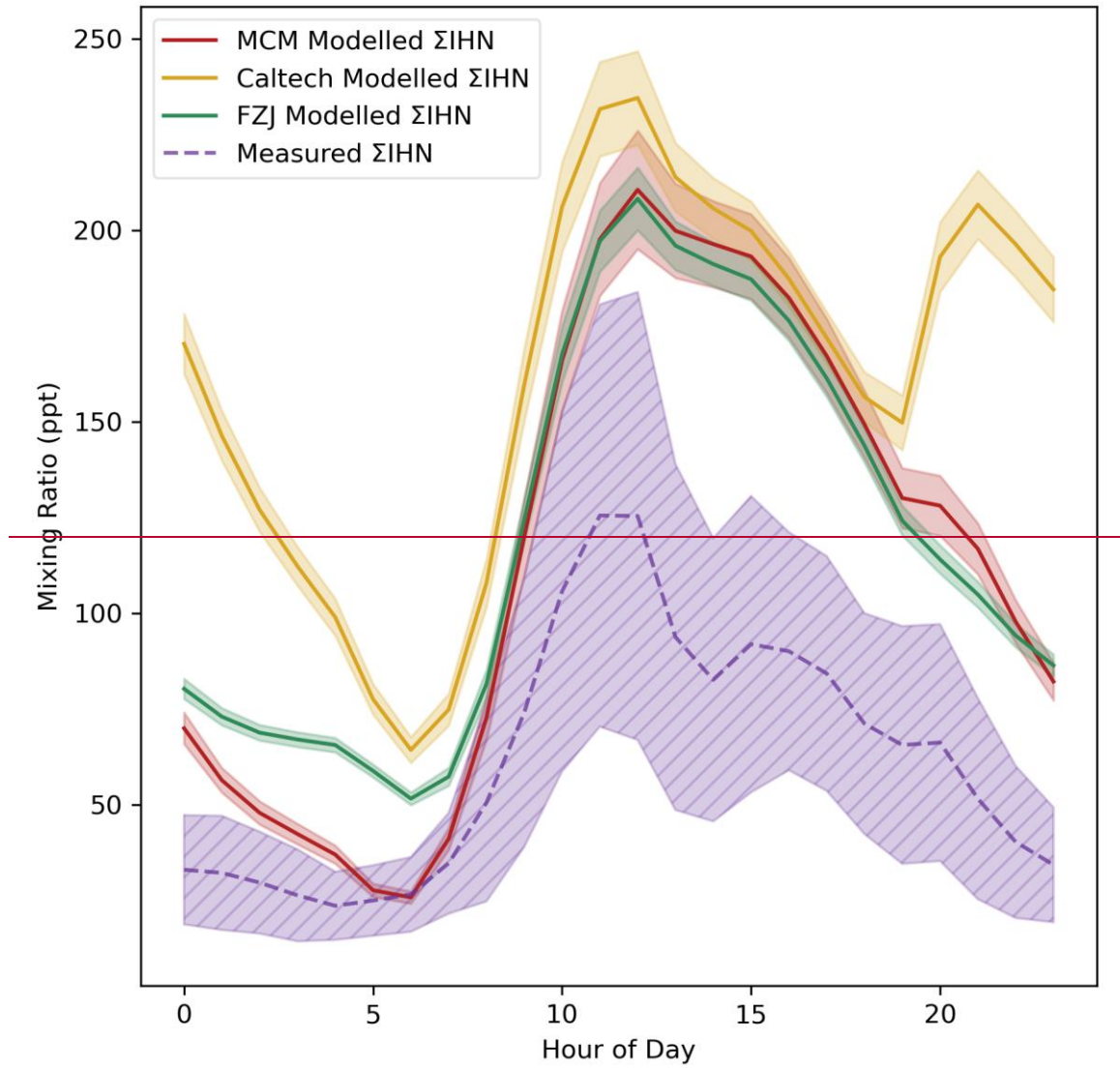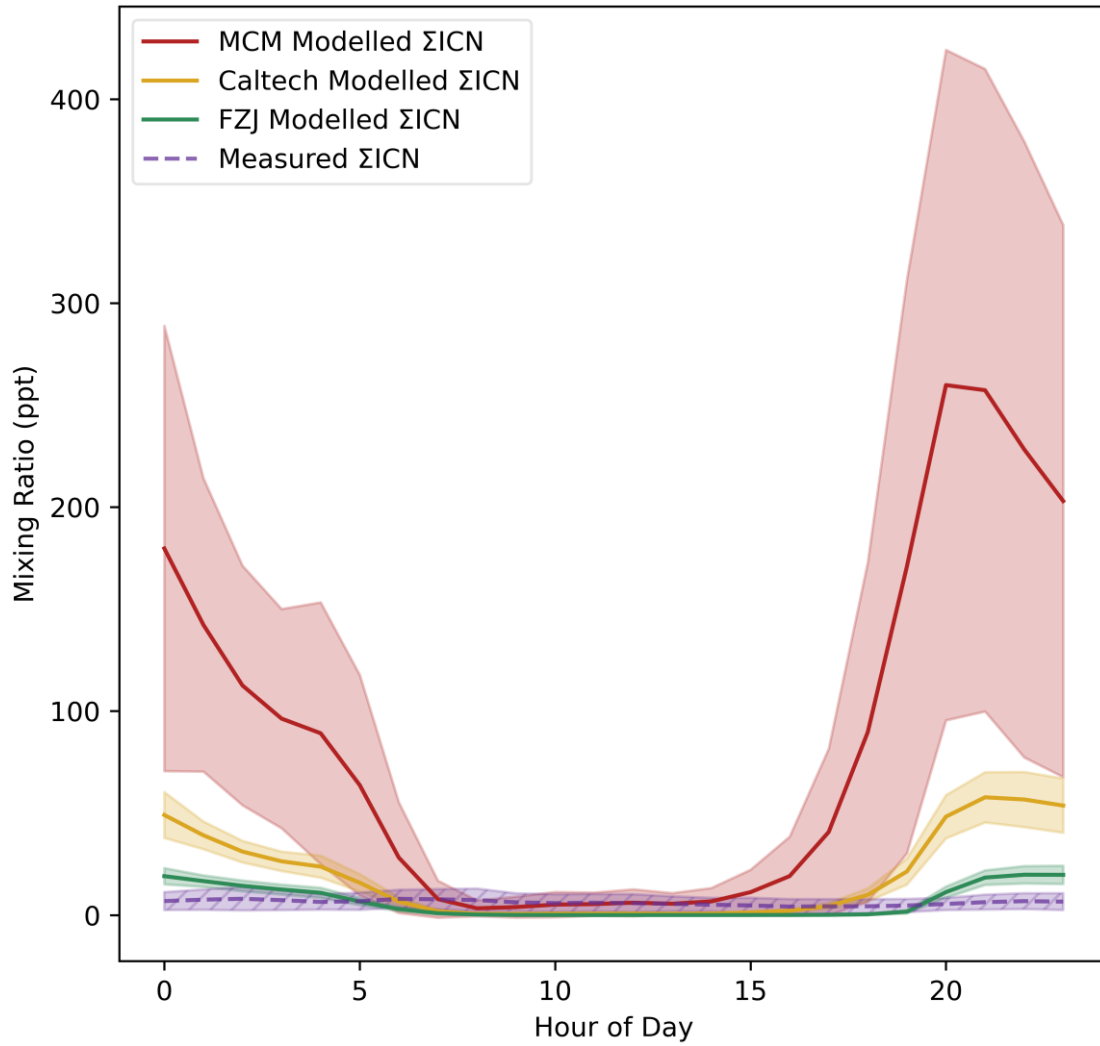
Figure 7. Measured and modelled ΣIHN. Each line shows the mean value for each dataset, with the shaded area indicating one standard deviation above and below the mean.
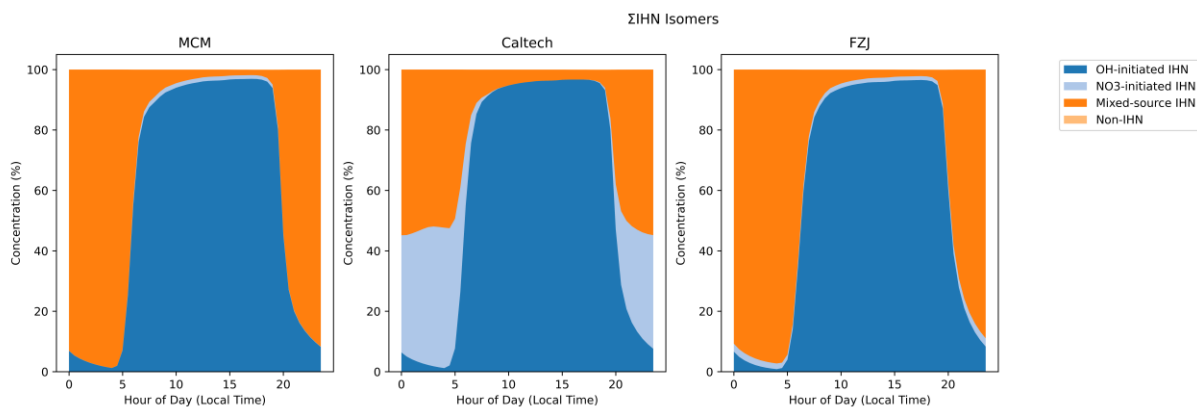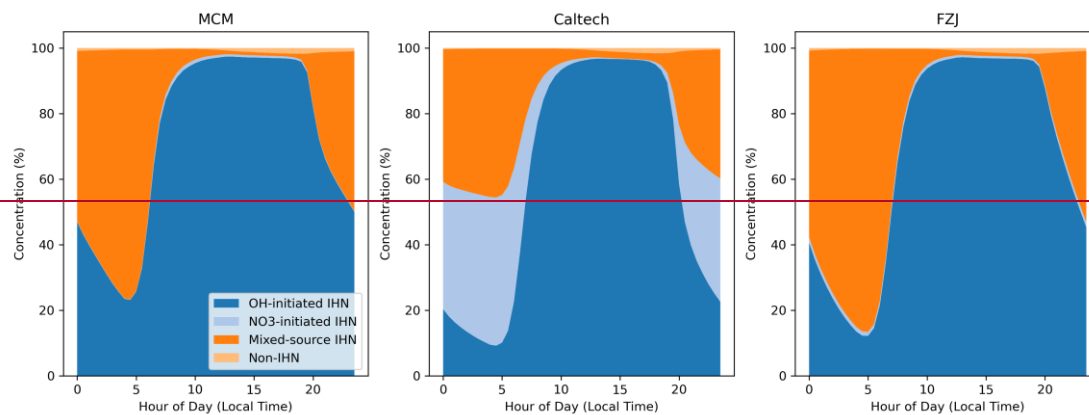
Figure 8. Isomer composition of the modelled ΣIHN. OH-initiated IHN are those primarily formed by OH chemistry, the 1,2-IHN and 4,3-IHN. NO3-initiated IHN are those primarily formed by NO3 chemistry, the 2,1-IHN and 3,4-IHN. Mixed-source IHN is formed in large amounts by both routes, the E/Z-1,4-IHN and E/Z-4,1-IHN.
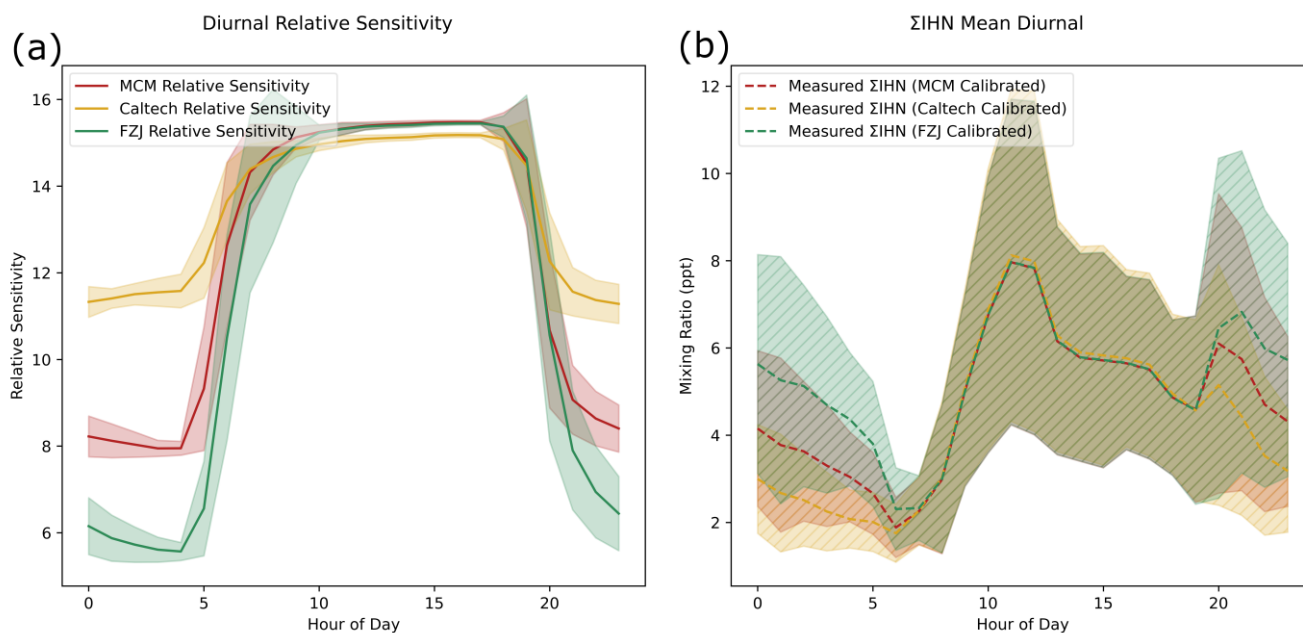
Figure 9. (a) Diurnal variation in the sensitivity of I⁻-CIMS to ΣIHN relative to IEPOX according to the isomer distribution predicted by each model. (b) The measured ΣIHN data adjusted using the relative sensitivity values from each mechanism.

33
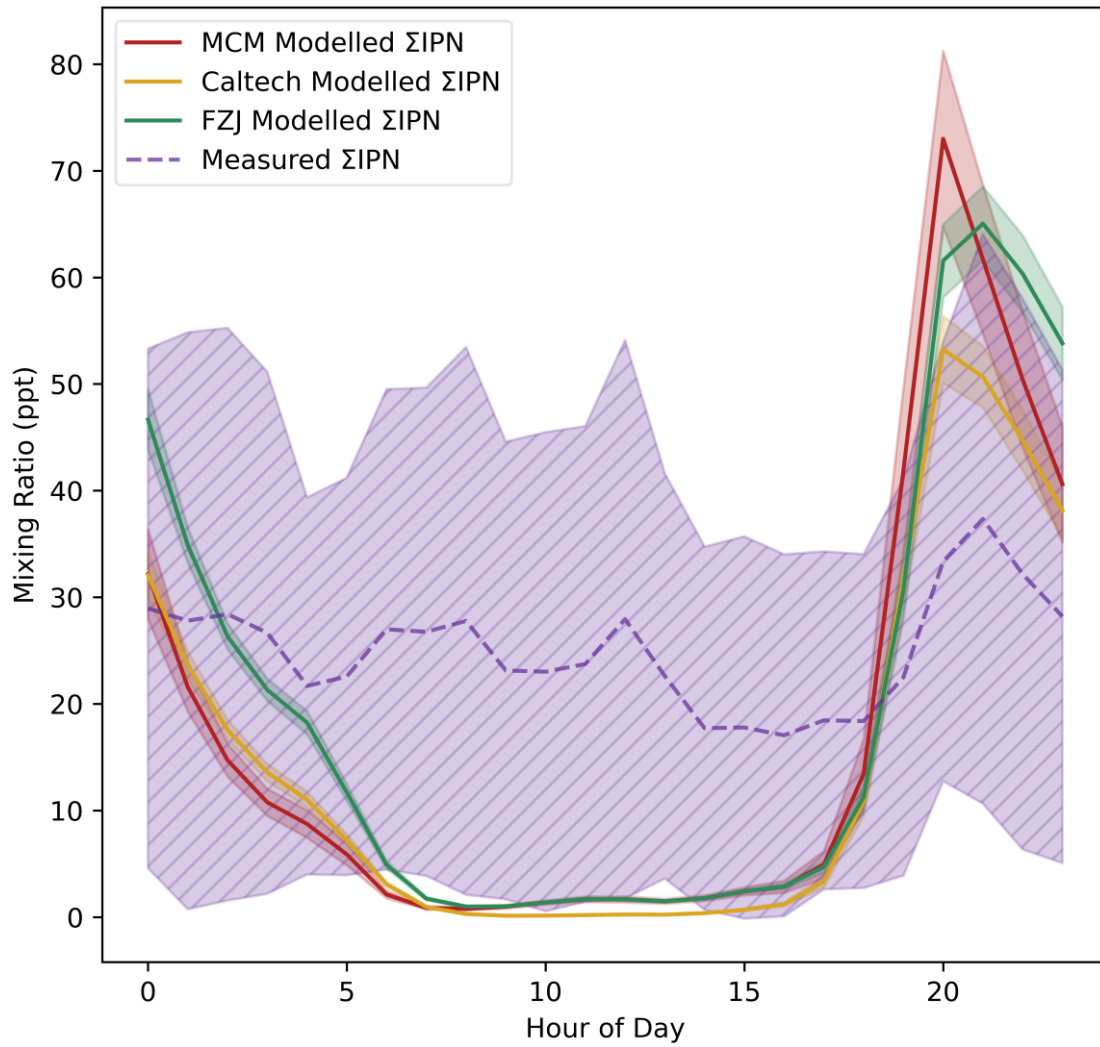
Figure 10. Measured and modelled ΣIPN (a). Each line shows the mean value for each dataset, with the shaded area indicating one standard deviation above and below the mean.
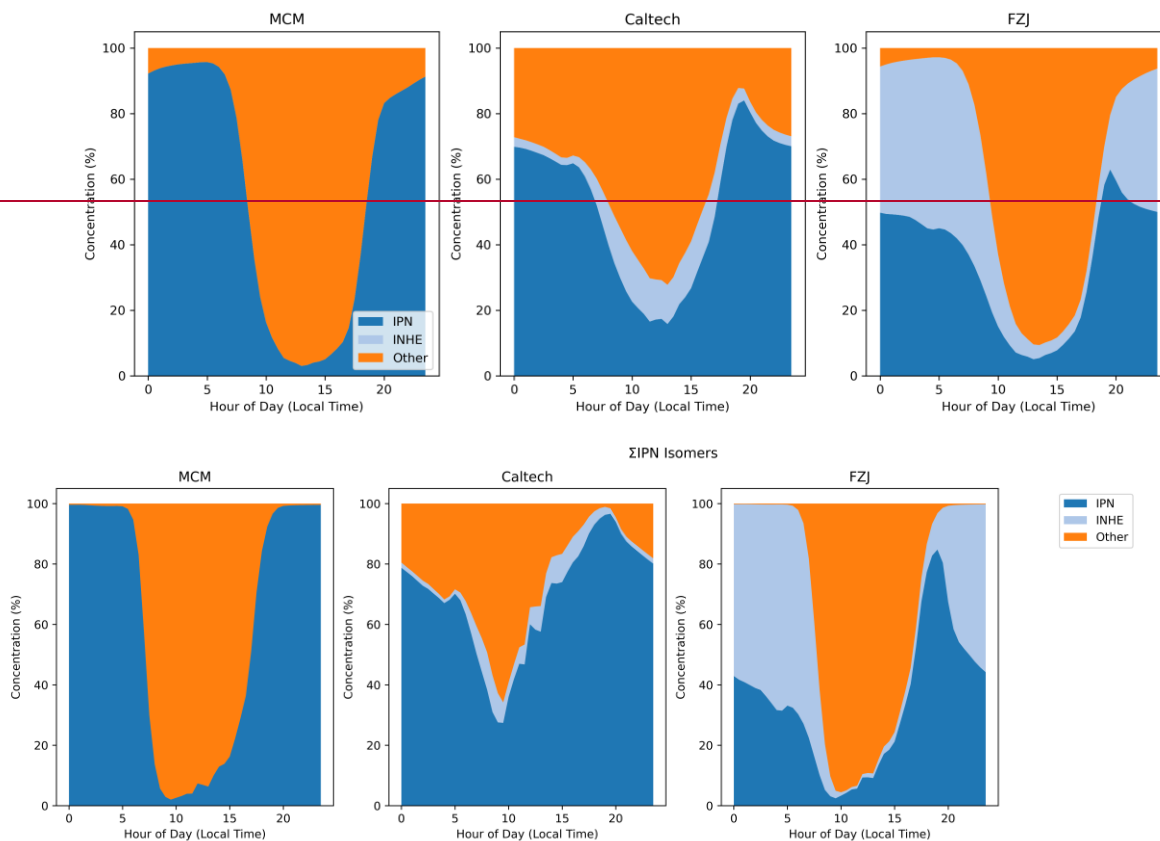
Figure 11. Isomer composition of the modelled ΣIPN as a percentage of total ΣIPN. "Other" comprises of ISOP1N253OH4OH, C530NO3, PPEN, C524NO3, C51NO3, and C5PAN4.

Figure 12.~~: Measured and modelled ΣIHN. Each line shows the mean value for each dataset, with the shaded area indicating one standard deviation above and below the mean.~~

Figure 10. Isomer composition of the modelled ΣIHN. OH-initiated IHN are those primarily formed by OH chemistry, the 1,2-IHN and 4,3-IHN. NO3-initiated IHN are those primarily formed by NO3 chemistry, the 2,1-IHN and 3,4-IHN. Mixed-source IHN is formed in large amounts by both routes, the E/Z-1,4-IHN and E/Z-4,1-IHN.
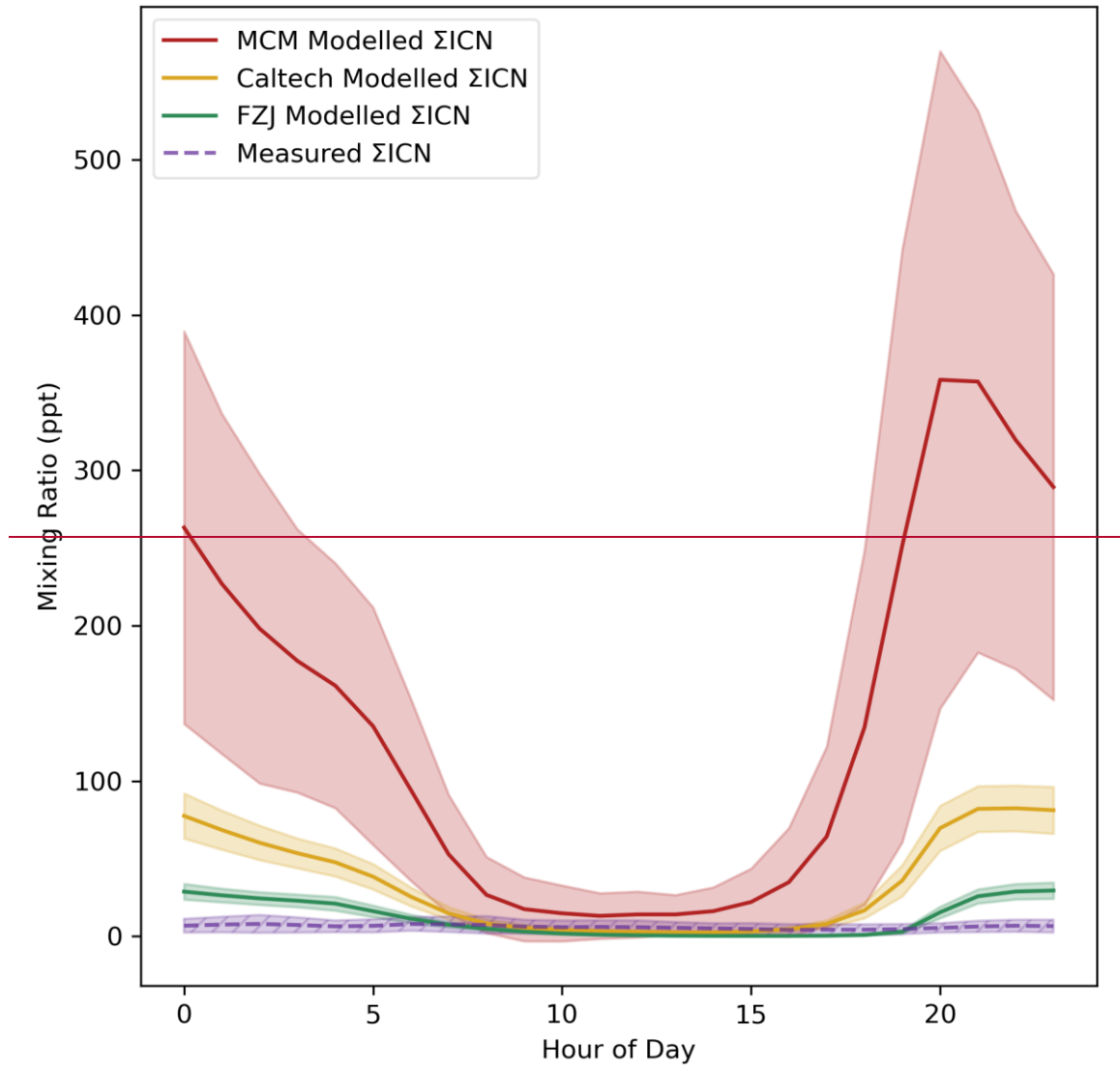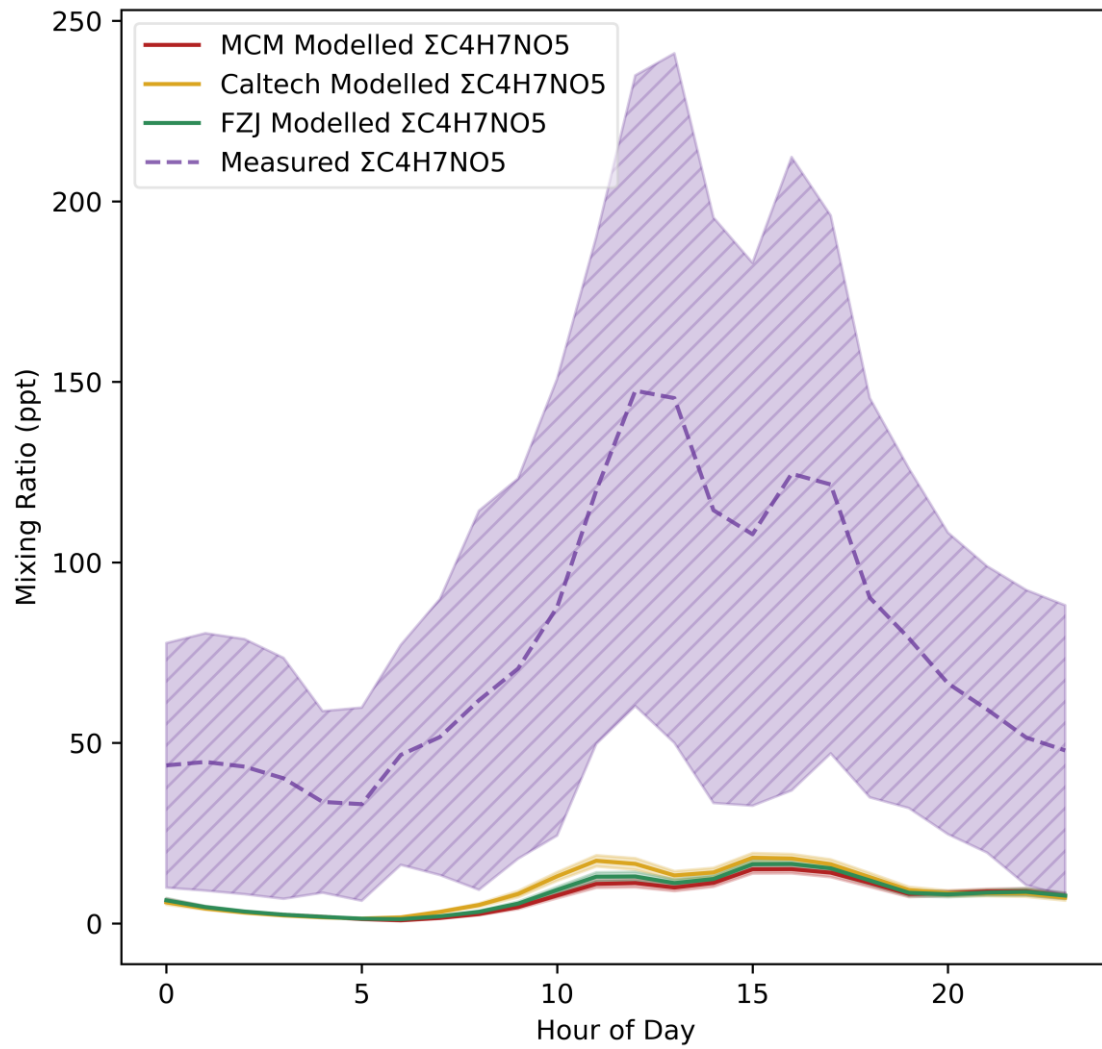
Figure 11. Measured and modelled ΣICN. Each line shows the mean value for each dataset, with the shaded area indicating one standard deviation above and below the mean.

970
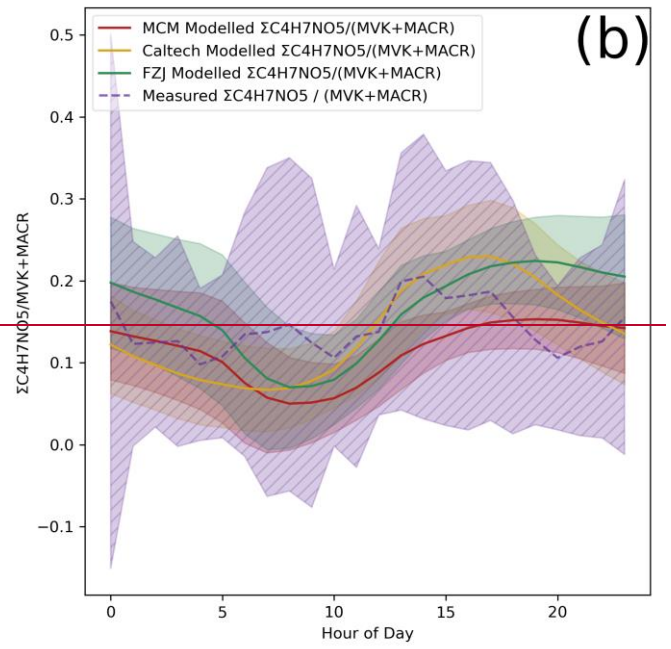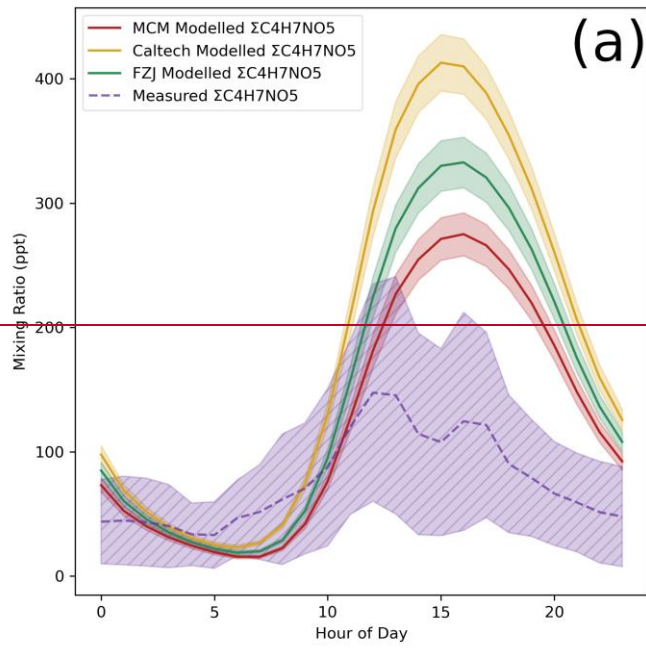
ΣC4H7NO5 Mean Diurnal

Figure 13. Measured and modelled ~~(a)~~ ΣC₄H₇NO₅ ~~and (b) ΣC₄H₇NO₅/(MVK+MACR).~~. Each line shows the mean value for each dataset, with the shaded area indicating one standard deviation above and below the mean.